Exploring the QGP at finite baryon chemical potential in and out of equilibrium

Elena Bratkovskaya

(GSI Darmstadt & Uni. Frankfurt)

Theoretical Physics Colloquium (on-line),

hosted by Prof. Igor Shovkovy at the Arizona State University.

20 January, 2021

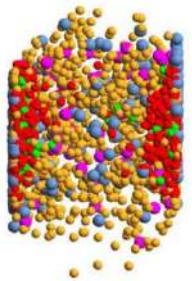

Experiment: Heavy-ion collisions

❑ Heavy-ion collision experiments

➔ ‚re-creation' of the Big Bang conditions in laboratory:
matter at high pressure and temperature

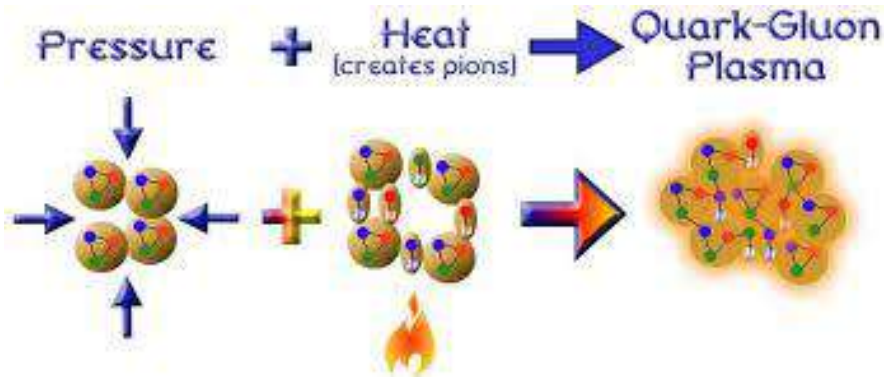

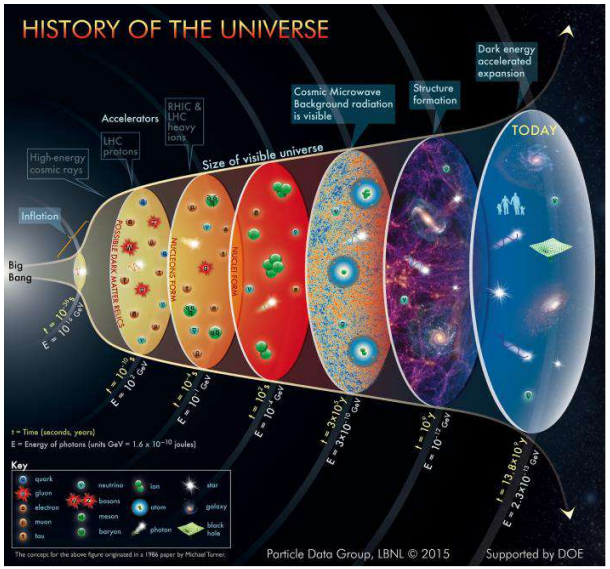

❑ Heavy-ion accelerators:

Large Hadron Collider - LHC (CERN):
Pb+Pb up to 574 A TeV

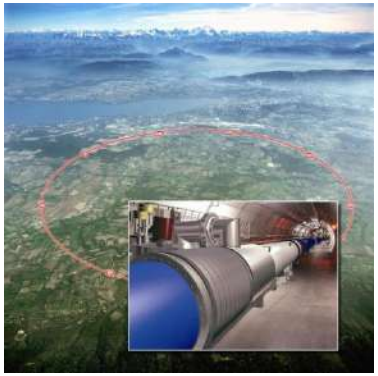

Relativistic-Heavy-Ion-Collider - RHIC (Brookhaven):
Au+Au up to 21.3 A TeV

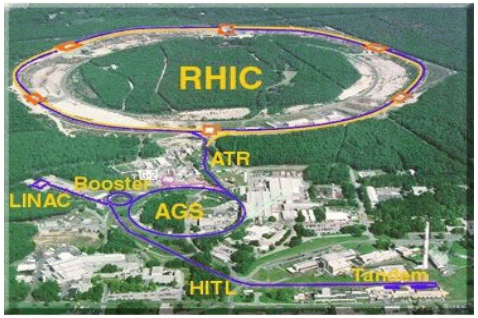

Facility for Antiproton and Ion Research – FAIR (Darmstadt)
(Under construction)
Au+Au up to 10 (30) A GeV

Nuclotron-based Ion Collider fAcility – NICA (Dubna)
(Under construction)
Au+Au up to 60 A GeV

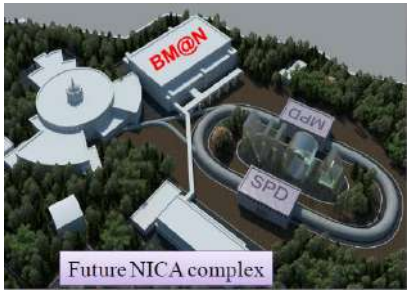

The ‚holy grail' of heavy-ion physics:

The phase diagram of QCD → thermal properties of QCD in the (T, μ_B) plain

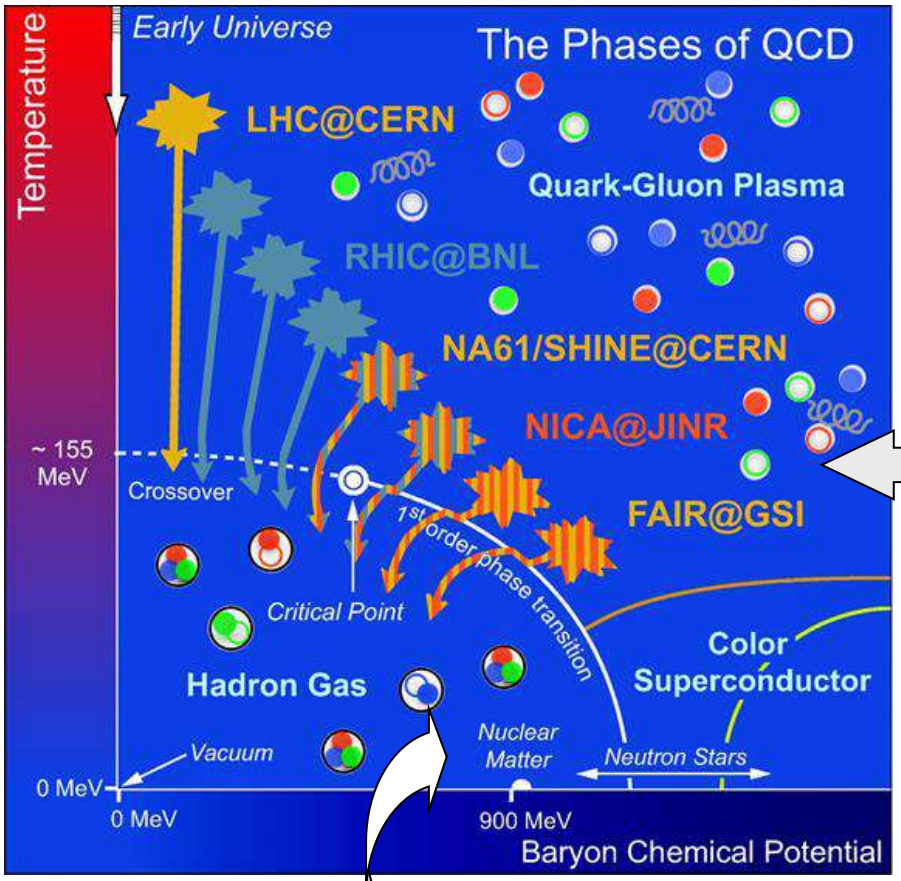

- **Equation-of-State of hot and dense matter?**
- **Study of the phase transition from hadronic to partonic matter – Quark-Gluon-Plasma**

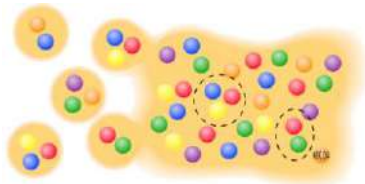

- **Search for a critical point**
- **Search for signatures of chiral symmetry restoration**
- **Study of the in-medium properties of hadrons at high baryon density and temperature**

Signals of the phase transition:

- Multi-strange particle enhancement in A+A
- Charm suppression
- Collective flow (v_1, v_2)
- Thermal dileptons
- Jet quenching and angular correlations
- High p_T suppression of hadrons
- Nonstatistical event-by-event fluctuations and correlations
- ...

Experiment: measures final hadrons and leptons

How to learn about physics from data?

Compare with theory!

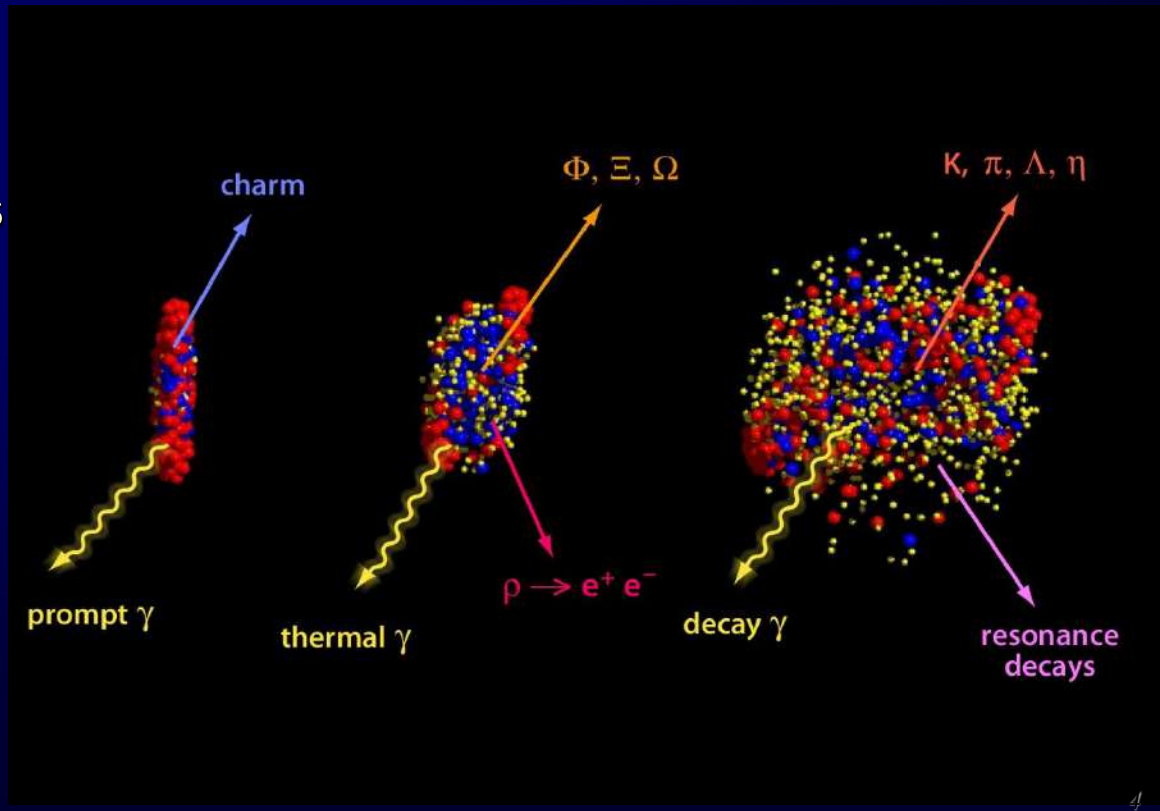

Basic models for heavy-ion collisions

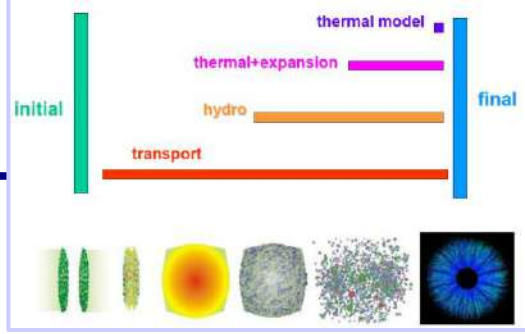

- **Statistical models:**

basic assumption: system is described by a (grand) canonical ensemble of non-interacting fermions and bosons in thermal and chemical equilibrium = thermal hadron gas at freeze-out with common T and μ_B

[- : no dynamical information]

- **Hydrodynamical models:**

basic assumption: conservation laws + equation of state (EoS); assumption of local thermal and chemical equilibrium

- Interactions are ‚hidden' in properties of the fluid described by transport coefficients (shear and bulk viscosity η, ζ, ..), which is 'input' for the hydro models

[- : simplified dynamics]

- **Microscopic transport models:**

based on transport theory of relativistic quantum many-body systems

- Explicitly account for the interactions of all degrees of freedom (hadrons and partons) in terms of cross sections and potentials

- Provide a unique dynamical description of strongly interaction matter in- and out-off equilibrium:

- In-equilibrium: transport coefficients are calculated in a box – controled by lQCD

- Nonequilibrium dynamics – controled by HIC

Actual solutions: Monte Carlo simulations

[+ : full dynamics | - : very complicated]

Microscopic modeling of HICs

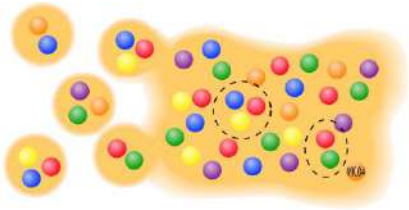

Goal: microscopic transport description of the partonic and hadronic phases of heavy-ion collisions

Problems:

- What are the properties of the QGP degrees of freedom?
- How to solve the hadronization problem?
- What is an appropriate transport theory ?

Information from lattice QCD at μ_B=0

I. deconfinement phase transition with increasing temperature

+

II. chiral symmetry restoration with increasing temperature

lQCD BMW collaboration: μ_B=0

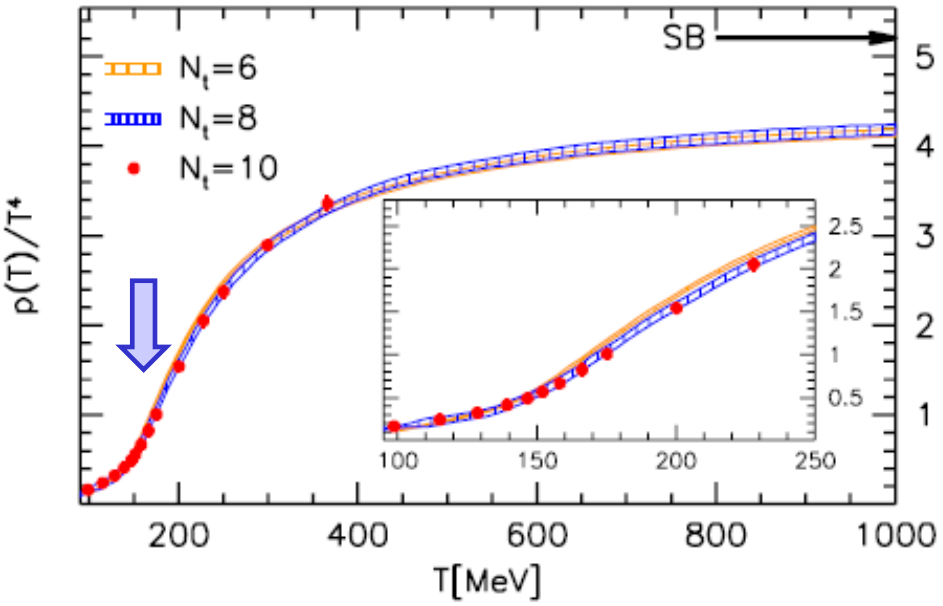

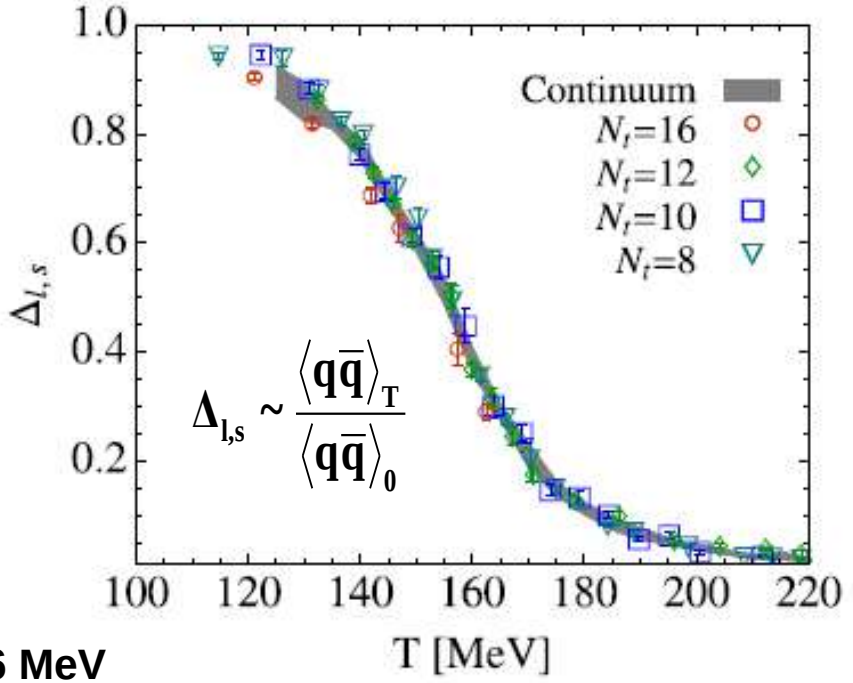

- **EoS: Crossover**: **hadron gas → QGP**, T_C =156 MeV

- **Scalar quark condensate $\langle \bar{q}q \rangle$ is viewed as an order parameter for the restoration of chiral symmetry:**

$$< \bar{q}q >= \begin{cases} \neq 0 & \text{chiral non-symmetric phase;} \\ = 0 & \text{chiral symmetric phase.} \end{cases}$$

→ **both transitions occur at about the same temperature T_C for low chemical potentials**

Thermodynamics of QCD at finite T and μ_B

Theory: → thermal properties of QCD in the (T, μ_B) plain
→ lattice QCD – limited to low μ_B < 400 MeV - 'sign problem' of lQCD at finite μ_B

Taylor expansion allows for lQCD calculations for $\mu_q/T << 1$ ($\mu_B=3\mu_q$)

lQCD: J. Guenther et al., Nucl. Phys. A 967 (2017) 720

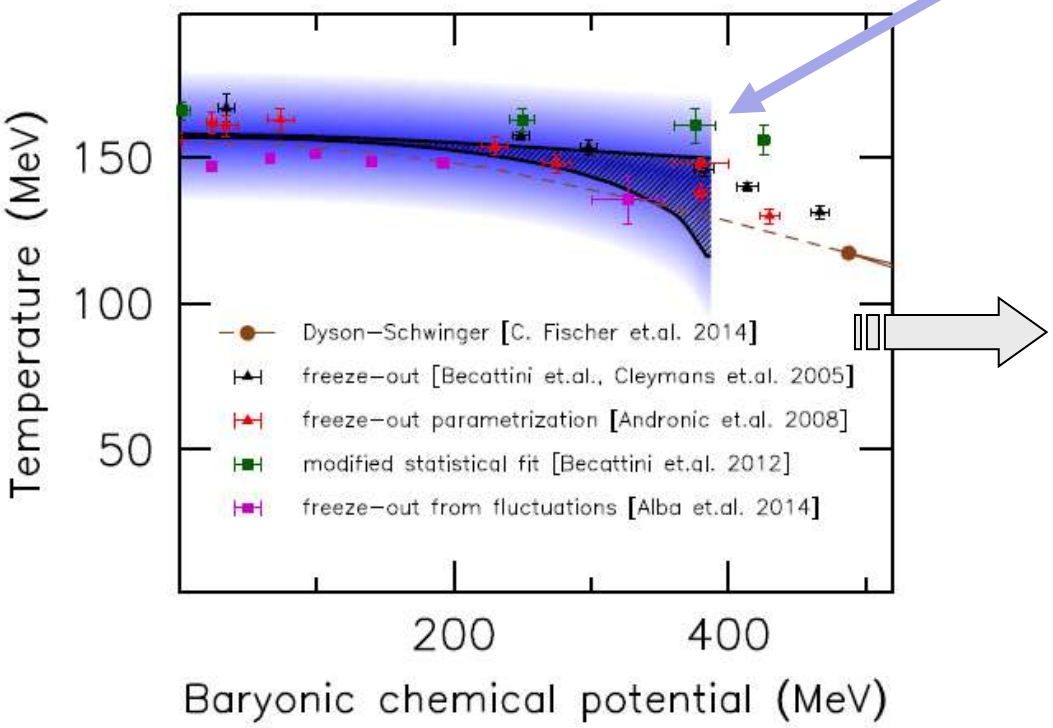

Possible phase diagram of QCD

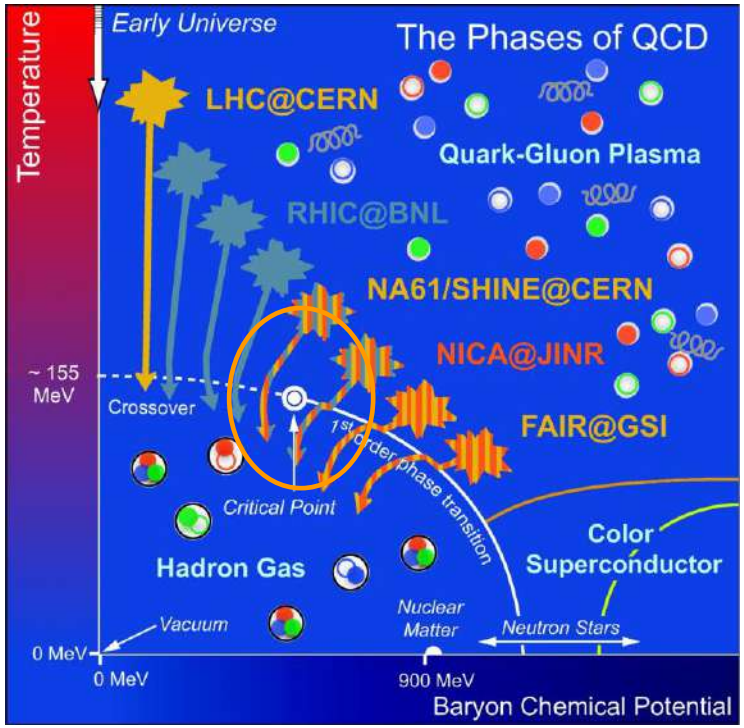

→ **Lattice QCD results: up to $\mu_B < 400\ MeV$:**

Crossover: hadron gas → QGP

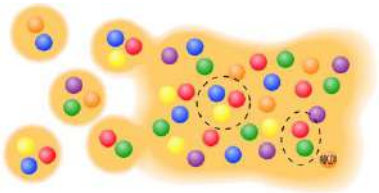

Degrees-of-freedom of the QGP

For the microscopic transport description of the system one needs to know all degrees of freedom as well as their properties and interactions!

- **lQCD gives QGP EoS at finite (T,μ_B)**

! needs to be interpreted in terms of degrees-of-freedom

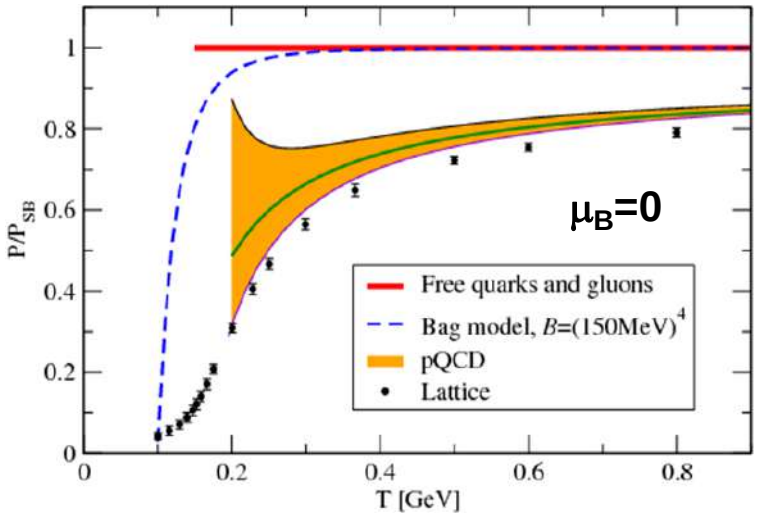

Non-perturbative QCD ← pQCD

pQCD:

- **weakly interacting system**
- **massless quarks and gluons**

Thermal QCD
= QCD at high parton densities:

- **strongly interacting system**
- **massive quarks and gluons**

➔ **quasiparticles**
= effective degrees-of-freedom

Present solution - effective models

DQPM (T, μ_q)

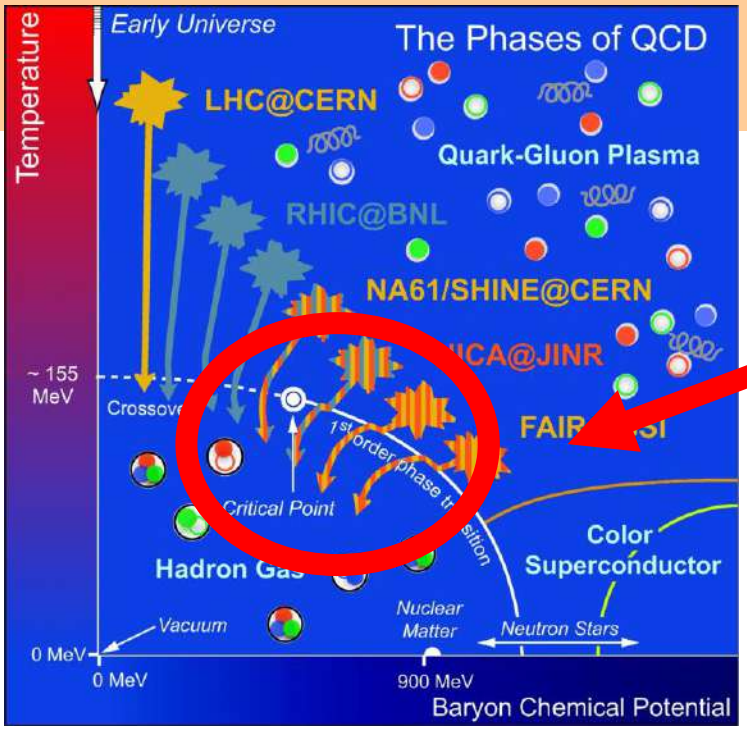

finite μ_q

Dynamical QuasiParticle Model (DQPM)

DQPM – effective model for the description of non-perturbative (strongly interacting) QCD based on lQCD EoS

Degrees-of-freedom: strongly interacting dynamical quasiparticles - quarks and gluons

Theoretical basis :

- **‚resummed' single-particle Green's functions ➔ quark (gluon) propagator (2PI) :**

gluon propagator: $\Delta^{-1} = P^2 - \Pi$ & quark propagator $S_q^{-1} = P^2 - \Sigma_q$

gluon self-energy: $\Pi = M_g^2 - i2\gamma_g\omega$ & quark self-energy: $\Sigma_q = M_q^2 - i2\gamma_q\omega$

Properties of the quasiparticles are specified by scalar complex self-energies:

$Re\Sigma_q$: **thermal masses** (M_g, M_q); $Im\Sigma_q$: **interaction widths** (γ_g, γ_q)

➔ **spectral functions** $\rho_q = -2ImS_q$ ➔ **Lorentzian form:**

$$\rho_j(\omega,\mathbf{p}) = \frac{\gamma_j}{\tilde{E}_j}\left(\frac{1}{(\omega-\tilde{E}_j)^2+\gamma_j^2} - \frac{1}{(\omega+\tilde{E}_j)^2+\gamma_j^2}\right)$$

$$\equiv \frac{4\omega\gamma_j}{\left(\omega^2-\mathbf{p}^2-M_j^2\right)^2+4\gamma_j^2\omega^2} \qquad \tilde{E}_j^2(\mathbf{p}) = \mathbf{p}^2 + M_j^2 - \gamma_j^2$$

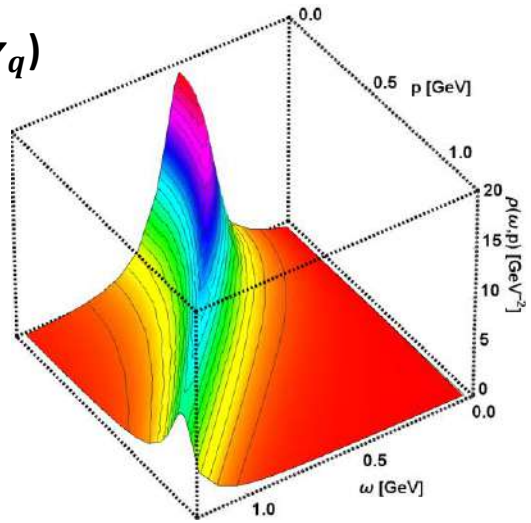

A. Peshier, W. Cassing, PRL 94 (2005) 172301; W. Cassing, NPA 791 (2007) 365: NPA 793 (2007), H. Berrehrah et al, Int.J.Mod.Phys. E25 (2016) 1642003; P. Moreau et al., PRC100 (2019) 014911; O. Soloveva et al., PRC101 (2020) 045203

Dynamical QuasiParticle Model (DQPM)

Theoretical basis → realization :

- introduce an ansatz (HTL; with few parameters) for the (T, μ_B) dependence of masses/widths
- ansatz for coupling constant *g* based on the lQCD entropy density as a function of T at μ_B=0
- scaling hypothesis for critical temperature $T_c(\mu_q)$:
- evaluate the QGP thermodynamics in equilibrium using the Kadanoff-Baym theory
- fix DQPM parameters by comparison to the entropy density s, pressure P, energy density ε from DQPM to lQCD results at μ_B =0

→ obtain the properties of the QGP at (T, μ_B)

A. Peshier, W. Cassing, PRL 94 (2005) 172301; W. Cassing, NPA 791 (2007) 365: NPA 793 (2007), H. Berrehrah et al, Int.J.Mod.Phys. E25 (2016) 1642003; P. Moreau et al., PRC100 (2019) 014911; O. Soloveva et al., PRC101 (2020) 045203

Parton properties

- **Modeling of the quark/gluon masses and widths (inspired by HTL calculations)**

Masses:

$$M^2_{q(\bar{q})}(T,\mu_B) = \frac{N_c^2-1}{8N_c} g^2(T,\mu_B)\left(T^2 + \frac{\mu_q^2}{\pi^2}\right)$$

$$M^2_{g}(T,\mu_B) = \frac{g^2(T,\mu_B)}{6}\left(\left(N_c + \frac{1}{2}N_f\right)T^2 + \frac{N_c}{2}\sum_q \frac{\mu_q^2}{\pi^2}\right)$$

Widths:

$$\gamma_{q(\bar{q})}(T,\mu_B) = \frac{1}{3}\frac{N_c^2-1}{2N_c}\frac{g^2(T,\mu_B)T}{8\pi}\ln\left(\frac{2c}{g^2(T,\mu_B)}+1\right)$$

$$\gamma_{g}(T,\mu_B) = \frac{1}{3}N_c\frac{g^2(T,\mu_B)T}{8\pi}\ln\left(\frac{2c}{g^2(T,\mu_B)}+1\right)$$

➔ **DQPM :**
only one parameter (c = 14.4) + (T, μ_B)- dependent coupling constant has to be determined from lattice results

- **Coupling g: input - lQCD entropy density s function of T at μ_B=0**

$$g^2(s/s_{SB}) = d\left((s/s_{SB})^e - 1\right)^f$$

$$s_{SB}^{QCD} = 19/9\pi^2 T^3$$

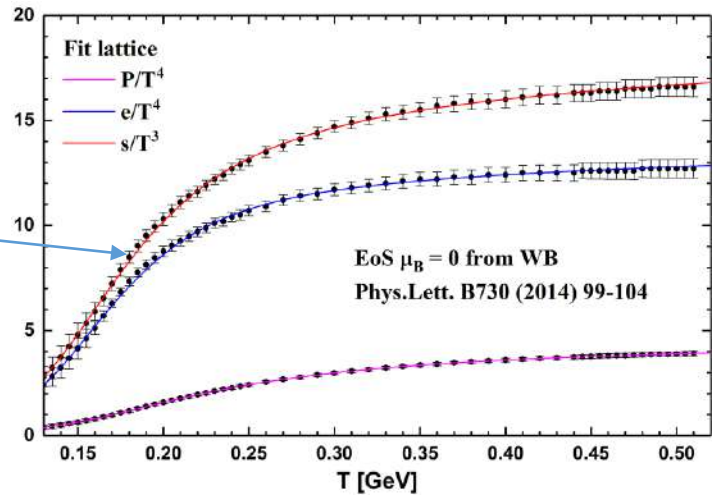

H. Berrehrah et al, PRC 93 (2016) 044914,
Int.J.Mod.Phys. E25 (2016) 1642003,

DQPM at finite (T, μ_q): scaling hypothesis

- **Scaling hypothesis for the effective temperature T***
  for $N_f = N_c = 3$

$$\mu_u = \mu_d = \mu_s = \mu_q$$

$$T^{*2} = T^2 + \frac{\mu_q^2}{\pi^2}$$

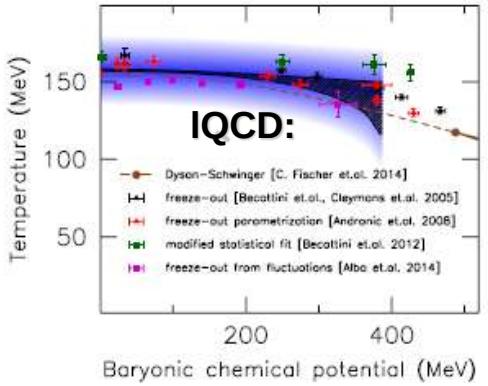

- **Coupling:**

$$g(T/T_c(\mu=0)) \longrightarrow g(T^*/T_c(\mu))$$

- **Critical temperature $T_c(\mu_q)$:**
  obtained by assuming a constant energy density ε for the system at $T=T_c(\mu_q)$, where ε at $T_c(\mu_q=0)=156$ GeV is fixed by lQCD at $\mu_q=0$

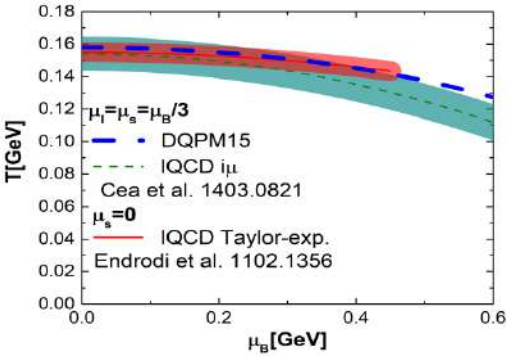

$$\frac{T_c(\mu_q)}{T_c(\mu_q=0)} = \sqrt{1-\alpha\,\mu_q^2} \approx 1 - \alpha/2\,\mu_q^2 + \cdots$$

$$\alpha \approx 8.79\ \mathrm{GeV}^{-2}$$

! Consistent with lattice QCD:

lQCD: C. Bonati et al., PRC90 (2014) 114025

$$\frac{T_c(\mu_B)}{T_c} = 1 - \kappa\left(\frac{\mu_B}{T_c}\right)^2 + \cdots$$

lQCD $\kappa = 0.013(2)$ $\longleftrightarrow$ $\kappa_{DQPM} \approx 0.0122$

H. Berrehrah et al, PRC 93 (2016) 044914, Int.J.Mod.Phys. E25 (2016) 1642003,

DQPM thermodynamics at finite (T, μ_q)

- **Entropy and baryon density in the quasiparticle limit (G. Baym 1998):**

$$s^{dqp} = -\int \frac{d\omega}{2\pi}\frac{d^3p}{(2\pi)^3}\Big[d_g\,\frac{\partial n_B}{\partial T}\left(\mathrm{Im}(\ln -\Delta^{-1}) + \mathrm{Im}\,\Pi\,\mathrm{Re}\,\Delta\right) + \sum_{q=u,d,s} d_q\,\frac{\partial n_F(\omega-\mu_q)}{\partial T}\left(\mathrm{Im}(\ln -S_q^{-1}) + \mathrm{Im}\,\Sigma_q\,\mathrm{Re}\,S_q\right) + \sum_{\bar{q}=\bar{u},\bar{d},\bar{s}} d_{\bar{q}}\,\frac{\partial n_F(\omega+\mu_q)}{\partial T}\left(\mathrm{Im}(\ln -S_{\bar{q}}^{-1}) + \mathrm{Im}\,\Sigma_{\bar{q}}\,\mathrm{Re}\,S_{\bar{q}}\right)\Big]$$

$$n^{dqp} = -\int \frac{d\omega}{2\pi}\frac{d^3p}{(2\pi)^3}\Big[\sum_{q=u,d,s} d_q\,\frac{\partial n_F(\omega-\mu_q)}{\partial \mu_q}\left(\mathrm{Im}(\ln -S_q^{-1}) + \mathrm{Im}\,\Sigma_q\,\mathrm{Re}\,S_q\right) + \sum_{\bar{q}=\bar{u},\bar{d},\bar{s}} d_{\bar{q}}\,\frac{\partial n_F(\omega+\mu_q)}{\partial \mu_q}\left(\mathrm{Im}(\ln -S_{\bar{q}}^{-1}) + \mathrm{Im}\,\Sigma_{\bar{q}}\,\mathrm{Re}\,S_{\bar{q}}\right)\Big]$$

Blaizot, Iancu, Rebhan, Phys. Rev. D 63 (2001) 065003

DQPM: P/T^4 ε/T^4 s/T^3 I/T^4

Input: lattice EoS $\mu_B = 0$

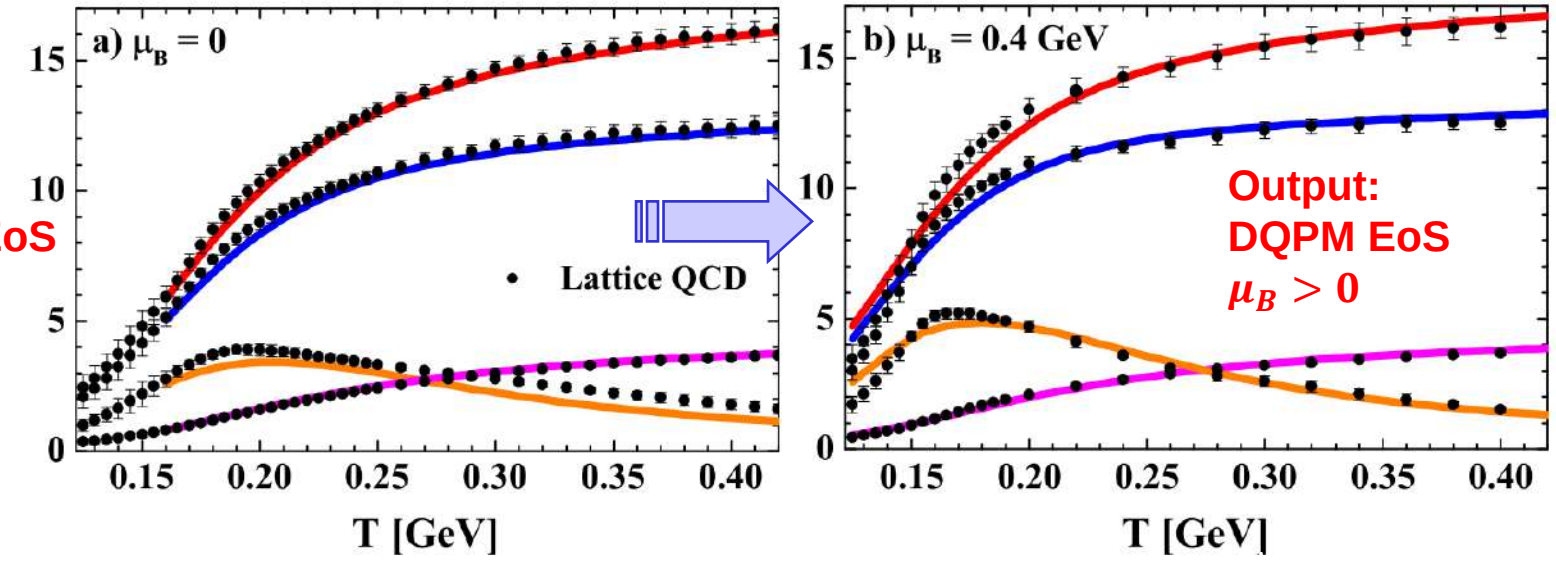

Output: DQPM EoS $\mu_B > 0$

lQCD: Sz. Borsanyi et al., JHEP 1208 (2012) 053

DQPM: parton properties

- **Coupling as a function of (T, μ_B)**

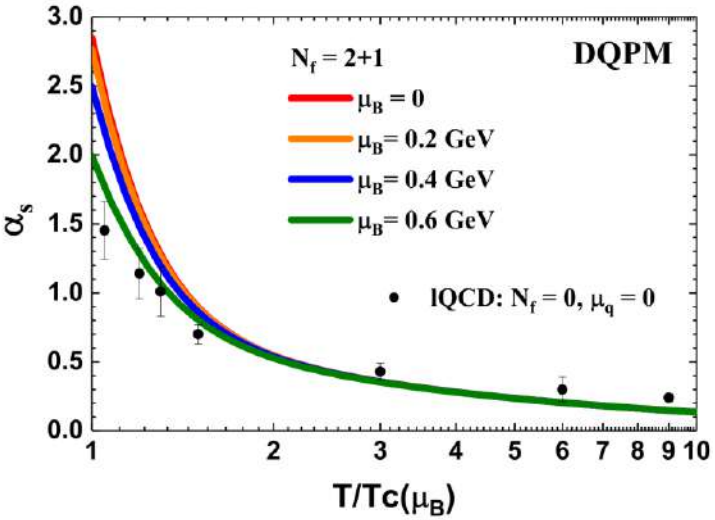

➔ **Lorentzian spectral function:**

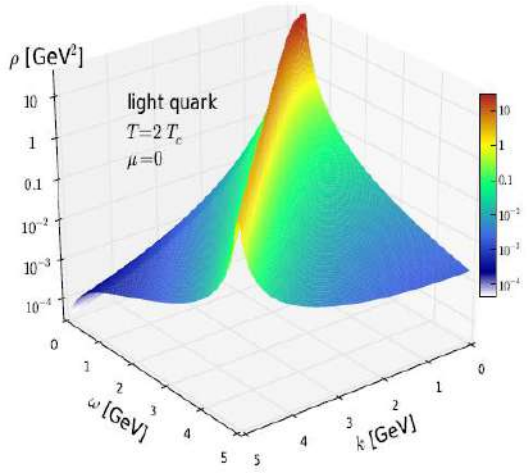

- **Masses and widths as a function of (T, μ_B)**

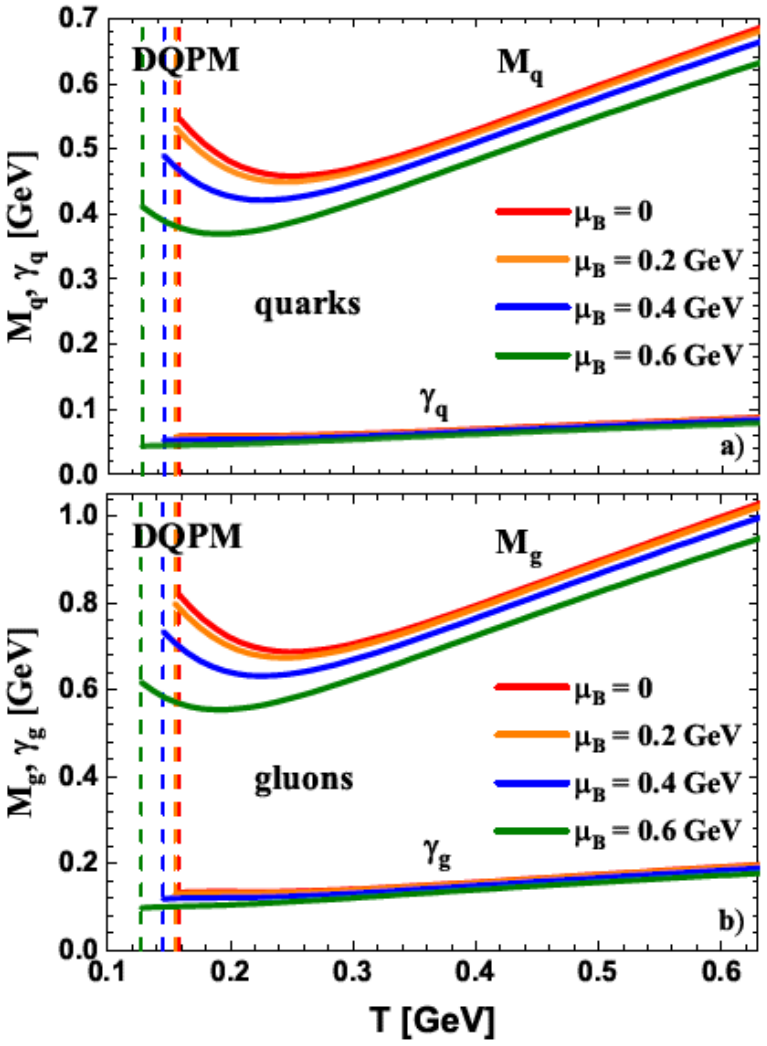

P. Moreau et al., PRC100 (2019) 014911

Partonic interactions: matrix elements

DQPM partonic cross sections → leading order diagrams

- **Propagators for massive bosons and fermions:**

$$\mu, a \quad \nu, b \quad q \qquad = -i\delta_{ab}\frac{g^{\mu\nu} - q^\mu q^\nu / M_g^2}{q^2 - M_g^2 + 2i\gamma_g q_0}$$

$$i \quad j \quad q \qquad = i\delta_{ij}\frac{\not{q} + M_q}{q^2 - M_q^2 + 2i\gamma_q q_0}$$

qq' → qq' scattering

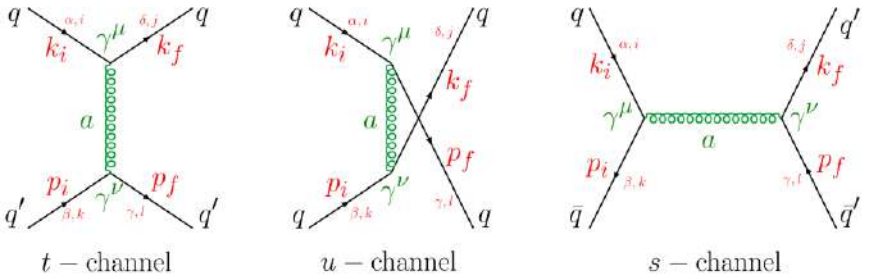

gq → gq scattering

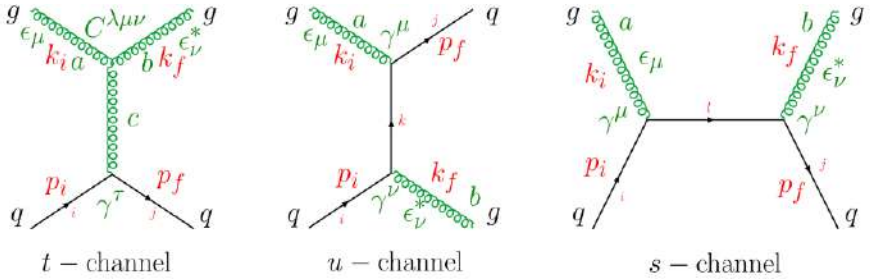

gg→ gg scattering

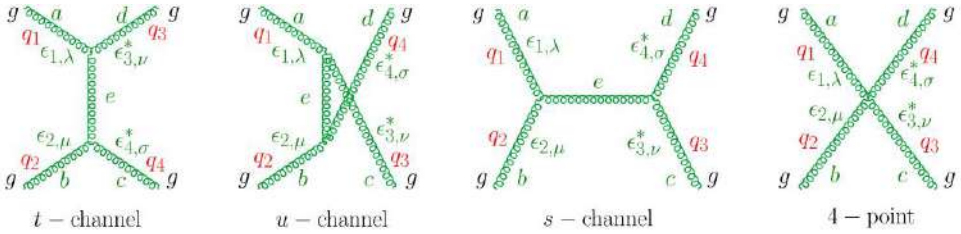

H. Berrehrah et al, PRC 93 (2016) 044914, Int.J.Mod.Phys. E25 (2016) 1642003,

P. Moreau et al., PRC100 (2019) 014911

Differential cross sections

☐ **On-shell:**

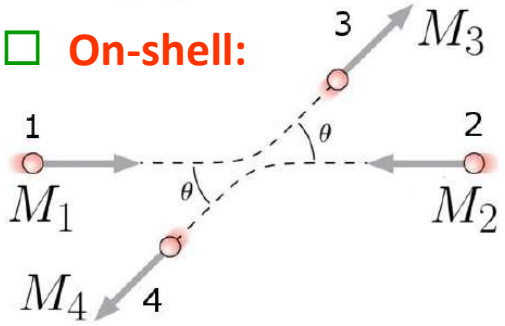

Initial masses: pole masses
Final masses: pole masses

❑ **Off-shell:**

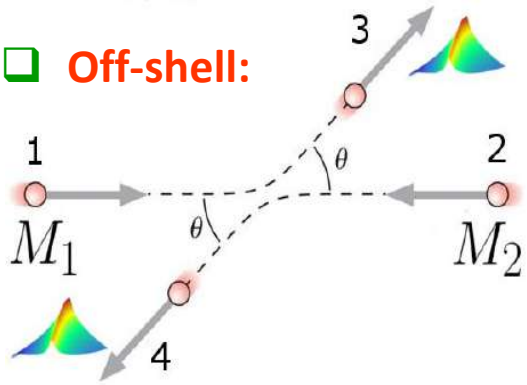

Initial masses: pole masses
Final masses: integrated over spectral functions

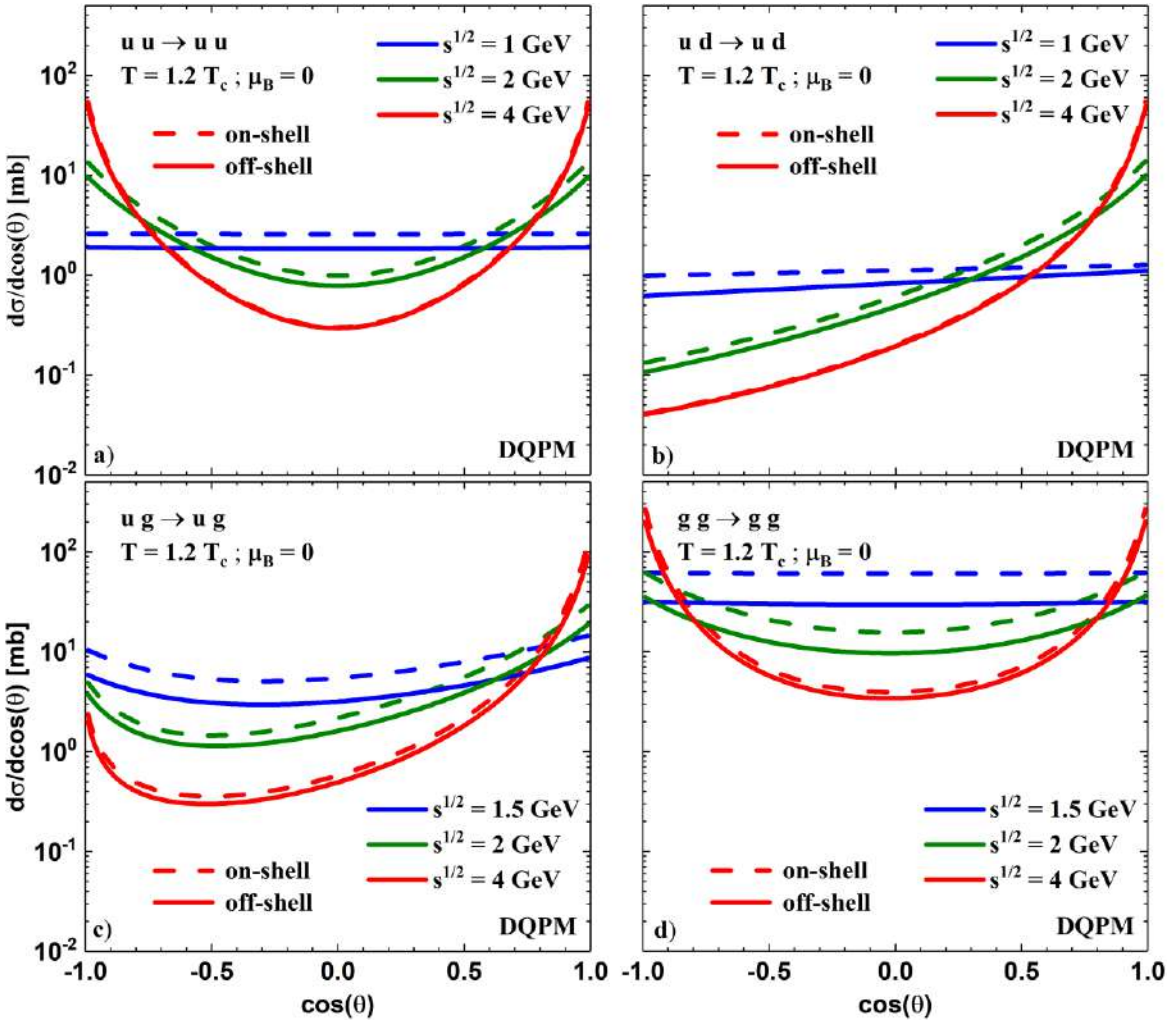

- **At lower s: off-shell σ < on -shell σ since $\omega_3 + \omega_4 < \sqrt{s}$**

P. Moreau et al., PRC100 (2019) 014911

Total cross section

- On-shell:

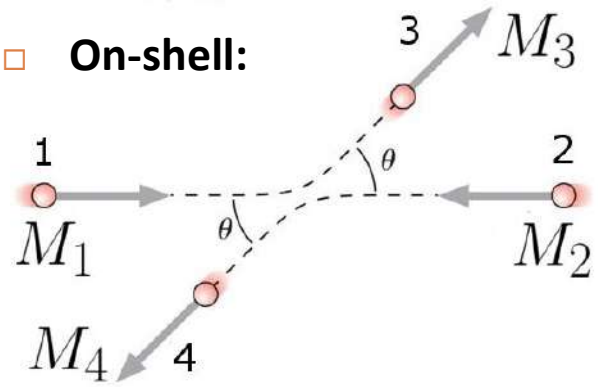

- Off-shell:

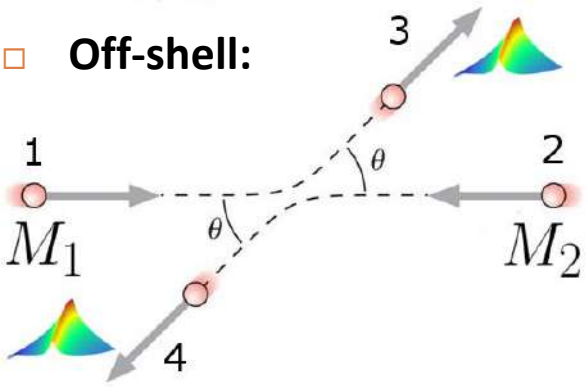

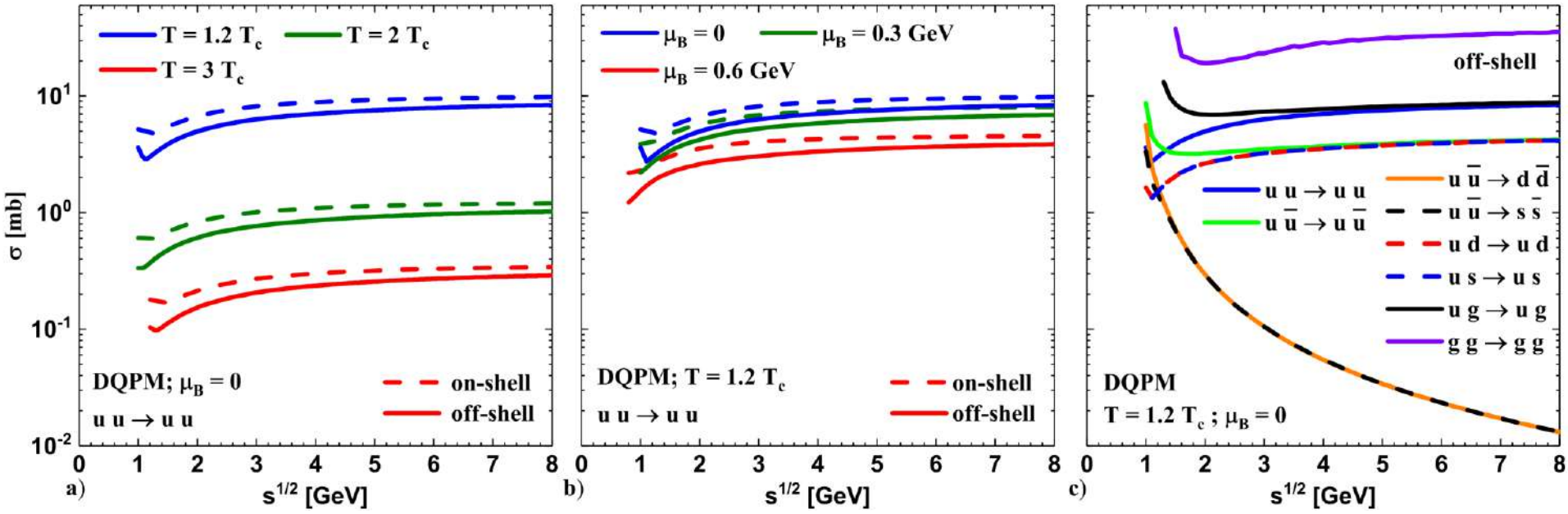

P. Moreau et al., PRC100 (2019) 014911

DQPM: Mean-field potential for quasiparticles

Space-like part of energy-momentum tensor $T_{\mu\nu}$ defines the potential energy density:

$$V_p(T,\mu_q) = T^{00}_{g-}(T,\mu_q) + T^{00}_{q-}(T,\mu_q) + T^{00}_{\bar{q}-}(T,\mu_q)$$

space-like gluons + space-like quarks+antiquarks

$$\tilde{T}r^{\pm}_{g} \cdots = d_g \int \frac{d\omega}{2\pi}\frac{d^3p}{(2\pi)^3}\, 2\omega\, \rho_g(\omega)\, \Theta(\omega)\, n_B(\omega/T)\; \Theta(\pm P^2) \cdots$$

$$\tilde{T}r^{\pm}_{q} \cdots = d_q \int \frac{d\omega}{2\pi}\frac{d^3p}{(2\pi)^3}\, 2\omega\, \rho_q(\omega)\, \Theta(\omega)\, n_F((\omega-\mu_q)/T)\; \Theta(\pm P^2) \cdots$$

$$\tilde{T}r^{\pm}_{\bar{q}} \cdots = d_{\bar{q}} \int \frac{d\omega}{2\pi}\frac{d^3p}{(2\pi)^3}\, 2\omega\, \rho_{\bar{q}}(\omega)\, \Theta(\omega)\, n_F((\omega+\mu_q)/T)\; \Theta(\pm P^2) \cdots$$

➔ **mean-field scalar potential (1PI) for quarks and gluons (U_q, U_g) vs parton scalar density ρ_S:**

$$U_s(\rho_s) = \frac{dV_p(\rho_s)}{d\rho_s} \qquad \rho_S = N_g^+ + N_q^+ + N_{\bar{q}}^+$$

$$Uq = Us, \;\; Ug \sim 2Us$$

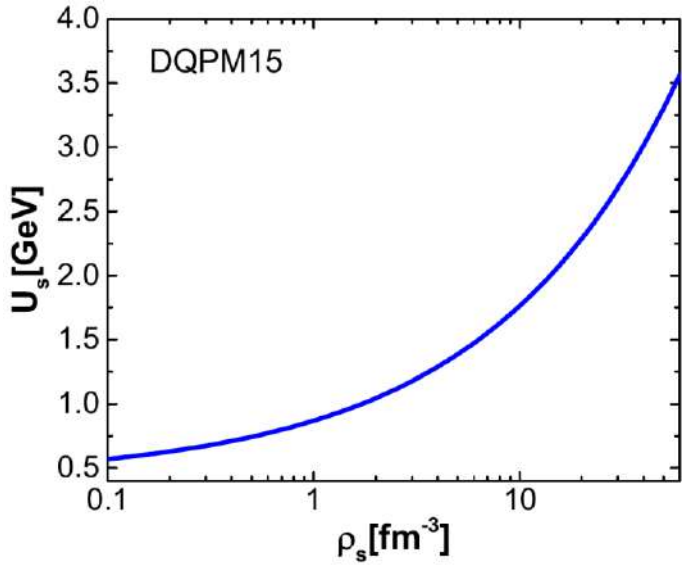

Quasiparticle potentials (U_q, U_g) are repulsive !

➔ **the force acting on a quasiparticle j:**

$$F \sim M_j/E_j \nabla U_s(x) = M_j/E_j \; dU_s/d\rho_s \; \nabla\rho_s(x)$$

$$j = g, q, \bar{q}$$

➔ **accelerates particles**

Cassing, NPA 791 (2007) 365: NPA 793 (2007)

QGP near equilibrium

DQPM (T, μ_q) :

transport properties at finite (T, μ_q)

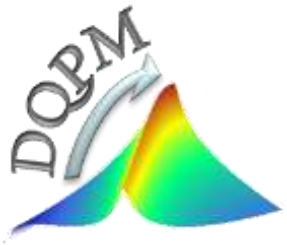

The properties of QGP in HICs → transport coefficients

Properties of the QGP near equilibrium are characterized by transport coefficients

Shear η, bulk viscosity ζ , … are 'input' for the viscous hydrodynamic models!

Hydrodynamics

$$T^{\mu\nu} = -Pg^{\mu\nu} + wu^\mu u^\nu + \Delta T^{\mu\nu}$$
$$J_B^\mu = n_B u^\mu + \Delta J_B^\mu$$

$$\begin{cases} \partial_\mu J_B^\mu = 0 \\ \partial_\mu T^{\mu\nu} = 0 \end{cases}$$

input for hydro simulations

$$\Delta T^{\mu\nu} = \eta\left(D^\mu u^\nu + D^\nu u^\mu + \tfrac{2}{3}\Delta^{\mu\nu}\partial_\rho u^\rho\right) - \zeta\Delta^{\mu\nu}\partial_\rho u^\rho$$
$$\Delta J_B^\mu = \kappa_B D^\mu\left(\frac{\mu_B}{T}\right)$$
$$D^\mu = \Delta^{\alpha\nu}\partial_\nu \qquad \Delta^{\mu\nu} = g^{\mu\nu} - u^\mu u^\nu$$

Shear viscosity
Resistance to 'deformation'
$\eta \bigtriangledown^{<\mu} u^{\nu>}$

Bulk viscosity
Resistance to expansion
$-\zeta \bigtriangledown u$

Baryon/electric charge
diffusion coefficients
$\kappa_B \bigtriangledown^\mu \frac{\mu_B}{T}$

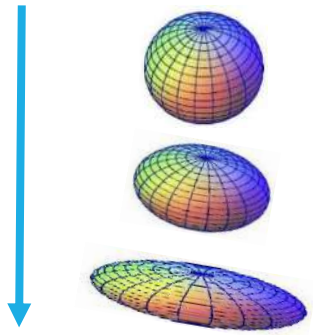

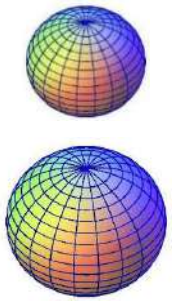

The properties of QGP from HIC - shear viscosity

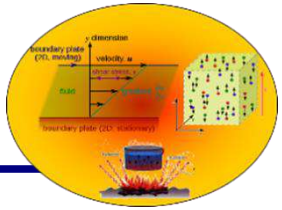

The shear viscosity of a system measures its resistance to flow.
Wikipedia: Viscosity can be conceptualized as quantifying the frictional force that arises between adjacent layers of fluid that are in relative motion.

Compilation of the ratio of shear viscosity to entropy density for various substances:

R. A. Lacey and A. Taranenko, PoS C FRNC2006, 021 (2006)

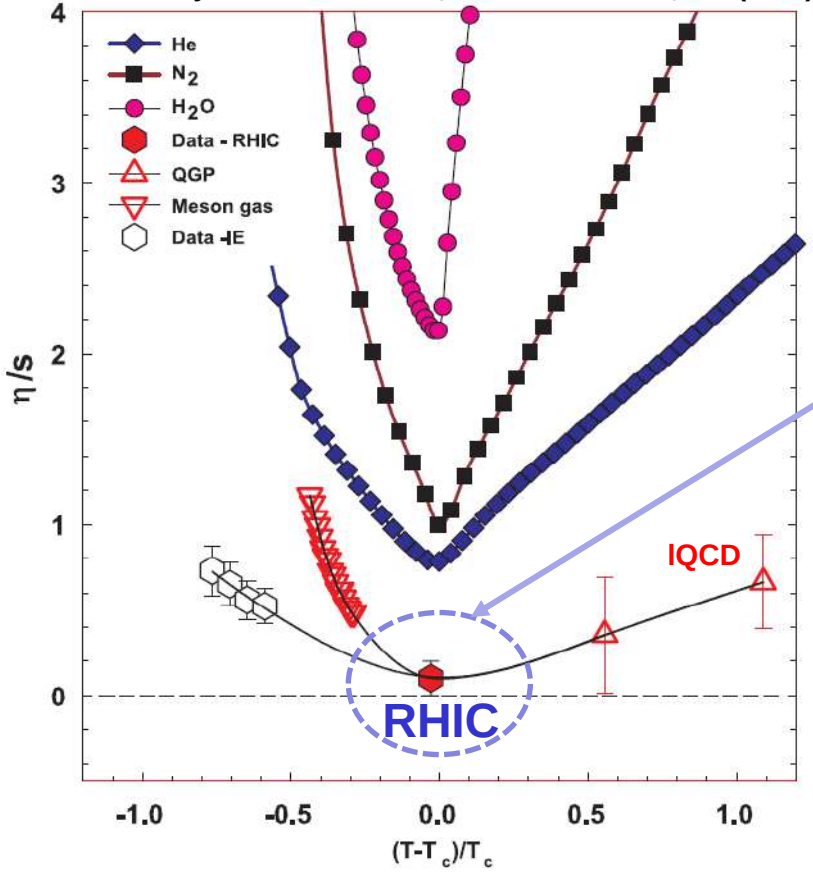

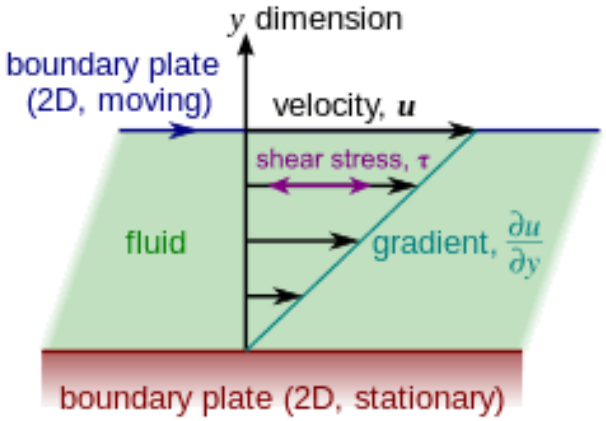

Exp. data + lQCD:
η/s near T_C is very small !

➔ QGP : close to an ideal liquid, not a gas of weakly interacting quarks and gluons

➔ QGP: strongly-interacting matter

pQCD: shear viscosity η

QCD: Pure Yang-Mills (only gluons)

LO (Leading order) perturbative QCD calculations:

η/s > 0.5 at T near T_C **'AMY':** P.B. Arnold, G.D. Moore and L.G. Yaffe,, JHEP 11 (2000) 001)

NLO (Next-to-leading order): (J. Ghiglieri, G.D. Moore, D. Teaney, JHEP 1803 (2018) 179):

"The next-to-leading order corrections are large and bring η/s down by more than a factor of 3 at physically relevant couplings.

The perturbative expansion is problematic even at T ~100 GeV"

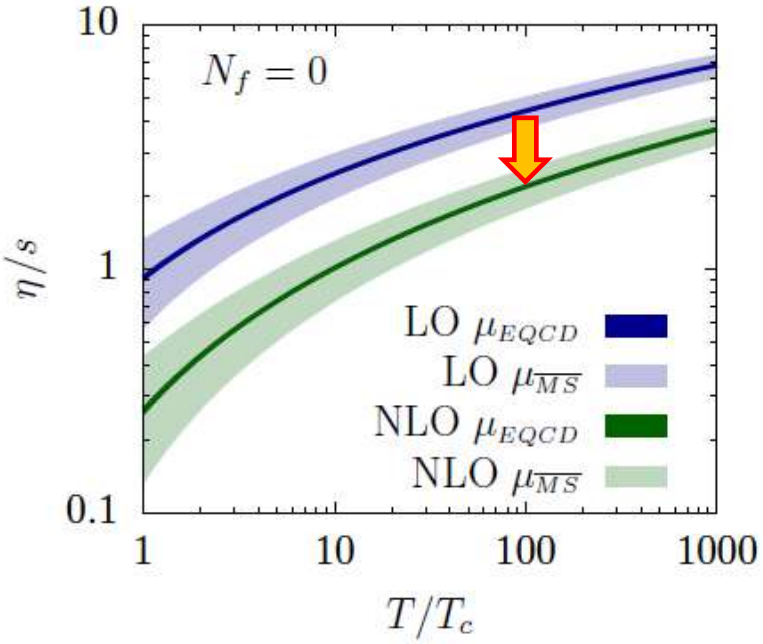

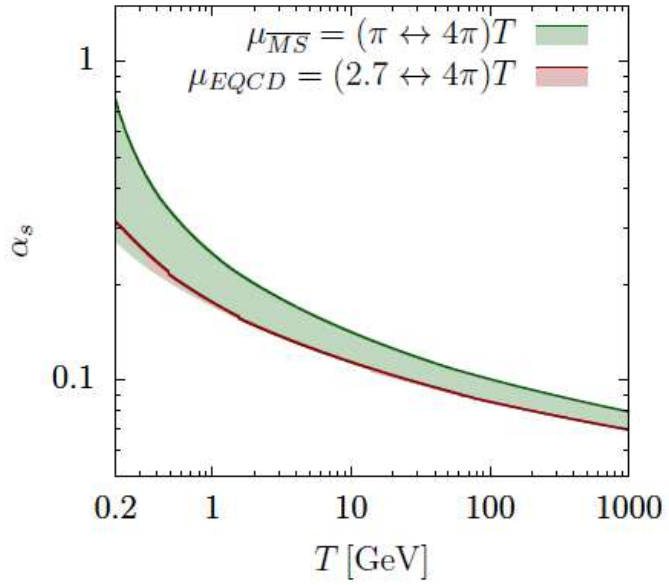

➔ **from pQCD to effective models of QCD!**

Transport coefficients: shear viscosity η

➢ Relaxation Time Approximation

$$\eta^{\mathrm{RTA}}(T,\mu_B) = \frac{1}{15T}\sum_{i=q,\bar{q},g}\int \frac{d^3p}{(2\pi)^3}\frac{\mathbf{p}^4}{E_i^2}\tau_i(\mathbf{p},T,\mu_B)\, d_i(1\pm f_i) f_i$$

$$1)\tau_i(\mathbf{p},T,\mu_B) = \frac{1}{\Gamma_i(\mathbf{p},T,\mu_B)}$$

$$2)\tau_i(T,\mu_B) = \frac{1}{2\gamma_i(T,\mu_B)},$$

η/s versus (T,μ_B)

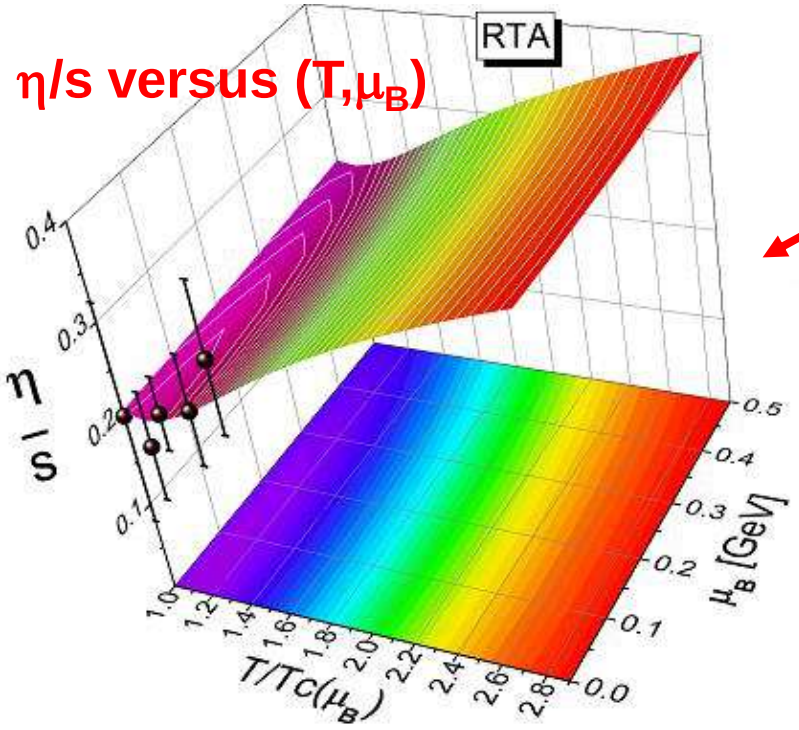

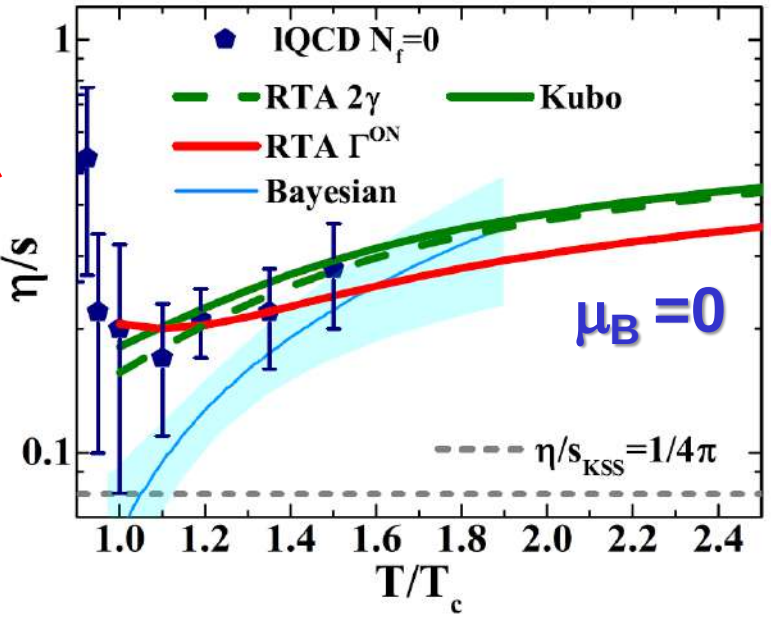

Hydro: Bayesian analysis, S. Bass et al. , NPA967 (2017) 67
Kovtun-Son-Starinets bound : $(\eta/s)_{KSS} = 1/(4\pi)$

➢ Weak dependence of shear viscosity on μ_B

Lattice QCD: N. Astrakhantsev et al, JHEP 1704 (2017) 101

P. Moreau et al., PRC100 (2019) 014911; O. Soloveva et al., PRC110 (2020) 045203

Transport coefficients: bulk viscosity ζ

➢ Relaxation Time Approximation

$$\zeta^{\mathrm{RTA}}(T,\mu_B) = \frac{1}{9T}\sum_{i=q,\bar{q},g}\int \frac{d^3p}{(2\pi)^3}\tau_i(\mathbf{p},T,\mu_B)$$

Relaxation times

$$\times\ \frac{d_i(1\pm f_i)f_i}{E_i^2}\left(\mathbf{p}^2 - 3c_s^2\left(E_i^2 - T^2\frac{dm_i^2}{dT^2}\right)\right)^2$$

From DQPM parametrization

Speed of sound

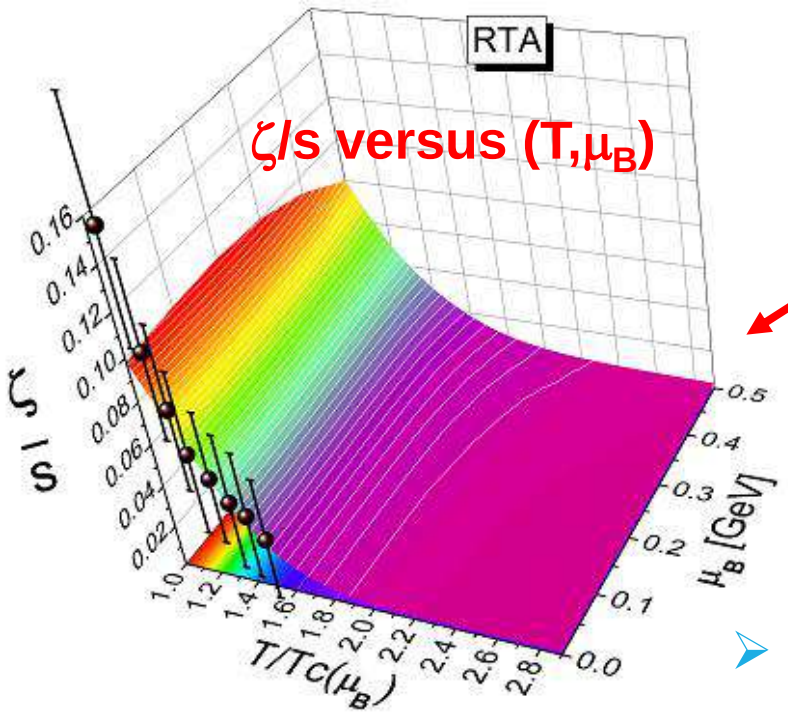

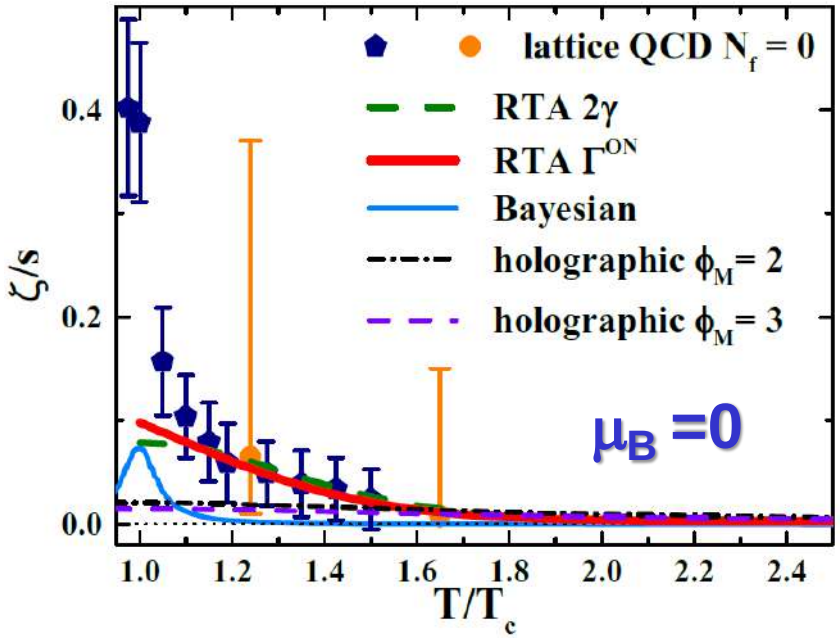

Lattice: Astrakhantsev et al, Phys.Rev. D98 (2018) 054515

➢ **Weak dependence of bulk viscosity on μ_B**

P. Moreau et al., PRC100 (2019) 014911; O. Soloveva et al., PRC110 (2020) 045203

Transport coefficients: electric conductivity σ_e/T

σ_0 ➔ **Probe of electric properties of the QGP**

η/s versus (T,μ_B)

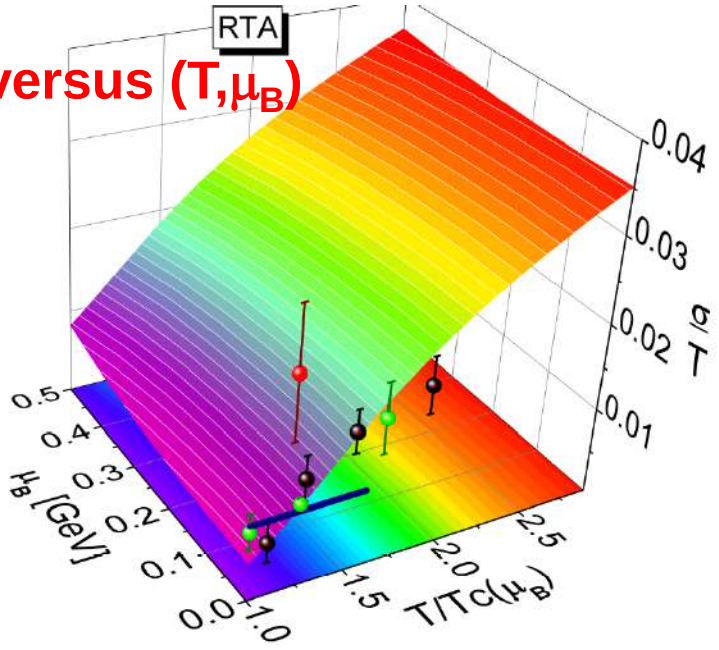

- **Relaxation Time Approximation**

$$\sigma_0^{\mathrm{RTA}}(T,\mu_B) = \frac{e^2}{3T}\sum_{i=q,\bar{q}} q_i^2 \int \frac{d^3p}{(2\pi)^3}\frac{\mathbf{p}^2}{E_i^2} \times \tau_i(\mathrm{p},T,\mu_B)\, d_i(1-f_i)f_i$$

- **the QCD matter even at T~ T_c is a much better electric conductor than Cu or Ag (at room temperature) by a factor of 500 !**

Exp. observables – photon and dilepton spectra

- **Photon emission: rates for $q_0 \to 0$ are related to electric conductivity σ_0**

$$q_0 \frac{dR}{d^4x\, d^3q}\bigg|_{q_0\to 0} = \frac{T}{4\pi^3}\sigma_0$$

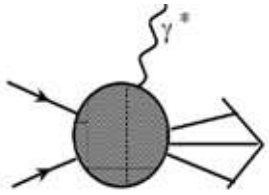

O. Soloveva et al., PRC110 (2020) 045203

Review: H. Berrehrah et al. Int.J.Mod.Phys. E25 (2016) 1642003

QGP:
in-equilibrium ➔ off-equilibrium

microscopic transport theory!

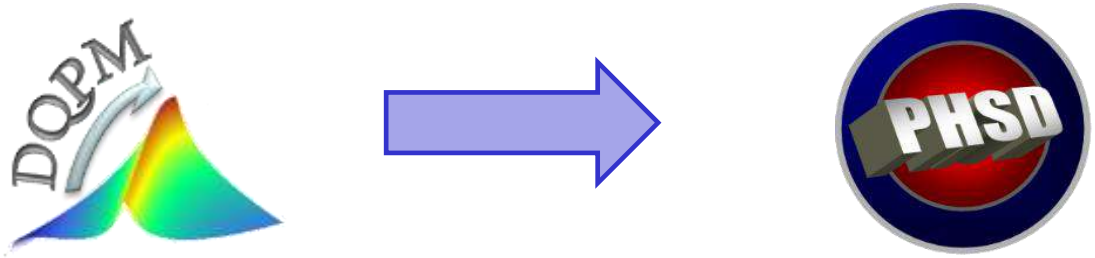

From weakly to strongly interacting systems

Properties of matter (on hadronic and partonic levels) **in heavy-ion collisions:**
QGP – strongly interacting system! Degrees of freedom – dressed partons!
Hadronic matter – in-medium effects – modification of hadron properties at finite T,μ_B (vector mesons, strange mesons)

Many-body theory:
Strong interaction ➔ large width = short life-time
➔ broad spectral function ➔ quantum object

- **How to describe the dynamics of broad strongly interacting quantum states in transport theory?**

❑ **semi-classical BUU**

first order gradient expansion of quantum Kadanoff-Baym equations

❑ **generalized transport equations based on Kadanoff-Baym dynamics**

Kbar* spectral function

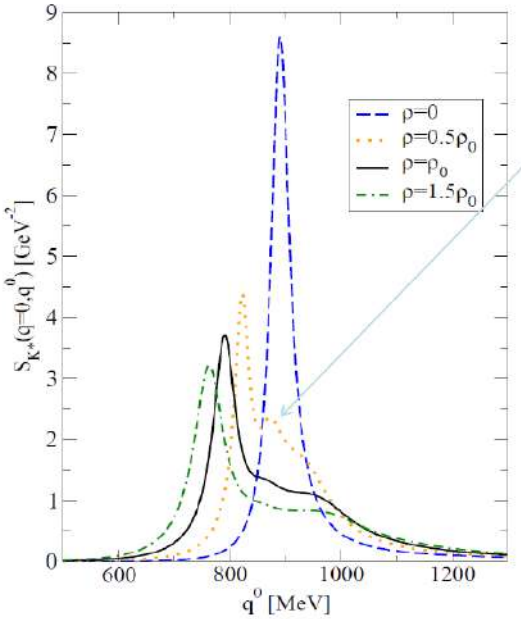

$\Lambda(1783)N^{-1}$ and $\Sigma(1830)N^{-1}$ exitations

Barcelona / Valencia group

Dynamical description of strongly interacting systems

❑ **Quantum field theory ➔**

Kadanoff-Baym dynamics for resummed single-particle Green functions $S^<$

$$\hat{S}_{0x}^{-1} S_{xy}^{<} = \Sigma_{xz}^{ret} \odot S_{zy}^{<} + \Sigma_{xz}^{<} \odot S_{zy}^{adv}$$

(1962)

Integration over the intermediate spacetime

Green functions $S^<$ / self-energies Σ:

$$iS_{xy}^{<} = \eta\langle\{\Phi^{+}(y)\Phi(x)\}\rangle$$

$$iS_{xy}^{>} = \langle\{\Phi(y)\Phi^{+}(x)\}\rangle$$

$$iS_{xy}^{c} = \langle T^{c}\{\Phi(x)\Phi^{+}(y)\}\rangle \quad -causal$$

$$iS_{xy}^{a} = \langle T^{a}\{\Phi(x)\Phi^{+}(y)\}\rangle \quad -anticausal$$

$$S_{xy}^{ret} = S_{xy}^{c} - S_{xy}^{<} = S_{xy}^{>} - S_{xy}^{a} \quad -retarded$$

$$S_{xy}^{adv} = S_{xy}^{c} - S_{xy}^{>} = S_{xy}^{<} - S_{xy}^{a} \quad -advanced$$

$$\eta = \pm 1 (bosons / fermions)$$

$$T^{a}(T^{c}) - (anti-)time-ordering\ operator$$

$$\hat{S}_{0x}^{-1} \equiv -(\partial_{x}^{\mu}\partial_{\mu}^{x} + M_{0}^{2})$$

Leo Kadanoff

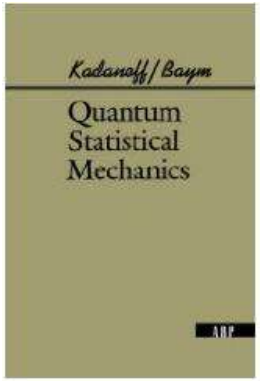

Gordon Baym

From Kadanoff-Baym equations to generalized transport equations

After the first order gradient expansion of the Wigner transformed Kadanoff-Baym equations and separation into the real and imaginary parts one gets:

Generalized transport equations (GTE):

drift term | Vlasov term | backflow term | collision term = ‚gain' - ‚loss' term

$$\diamond\{P^2 - M_0^2 - Re\Sigma^{ret}_{XP}\}\{S^<_{XP}\} - \diamond\{\Sigma^<_{XP}\}\{ReS^{ret}_{XP}\} = \frac{i}{2}[\Sigma^>_{XP}S^<_{XP} - \Sigma^<_{XP}S^>_{XP}]$$

Backflow term incorporates the off-shell behavior in the particle propagation
! vanishes in the quasiparticle limit $A_{XP} \rightarrow \delta(p^2\text{-}M^2)$

- **GTE: Propagation of the Green's function $iS^<_{XP}=A_{XP}N_{XP}$, which carries information not only on the number of particles (N_{XP}), but also on their properties, interactions and correlations (via A_{XP})**

- **Spectral function:**

$$A_{XP} = \frac{\Gamma_{XP}}{(P^2 - M_0^2 - Re\Sigma^{ret}_{XP})^2 + \Gamma^2_{XP}/4}$$

$\Gamma_{XP} = -Im\,\Sigma^{ret}_{XP} = 2\,p_0\Gamma$ – **‚width' of spectral function**
= reaction rate of particle (at space-time position X)

4-dimentional generalizaton of the Poisson-bracket:

$$\diamond\{F_1\}\{F_2\} := \frac{1}{2}\left(\frac{\partial F_1}{\partial X_\mu}\frac{\partial F_2}{\partial P^\mu} - \frac{\partial F_1}{\partial P_\mu}\frac{\partial F_2}{\partial X^\mu}\right)$$

- **Life time** $\tau = \frac{\hbar c}{\Gamma}$

W. Cassing , S. Juchem, NPA 665 (2000) 377; 672 (2000) 417; 677 (2000) 445

General testparticle off-shell equations of motion

W. Cassing , S. Juchem, NPA 665 (2000) 377; 672 (2000) 417; 677 (2000) 445

- Employ testparticle Ansatz for the real valued quantity $i\,S^{<}_{XP}$

$$F_{XP} = A_{XP}N_{XP} = i\,S^{<}_{XP} \sim \sum_{i=1}^{N} \delta^{(3)}(\vec{X} - \vec{X}_i(t))\;\delta^{(3)}(\vec{P} - \vec{P}_i(t))\;\delta(P_0 - \epsilon_i(t))$$

insert in generalized transport equations and determine equations of motion !

➔ **General testparticle Cassing's off-shell equations of motion for the time-like particles:**

$$\frac{d\vec{X}_i}{dt} = \frac{1}{1-C_{(i)}}\frac{1}{2\epsilon_i}\left[2\,\vec{P}_i + \vec{\nabla}_{P_i} Re\Sigma^{ret}_{(i)} + \frac{\epsilon_i^2 - \vec{P}_i^2 - M_0^2 - Re\Sigma^{ret}_{(i)}}{\Gamma_{(i)}}\vec{\nabla}_{P_i}\Gamma_{(i)}\right],$$

$$\frac{d\vec{P}_i}{dt} = -\frac{1}{1-C_{(i)}}\frac{1}{2\epsilon_i}\left[\vec{\nabla}_{X_i} Re\Sigma^{ret}_{i} + \frac{\epsilon_i^2 - \vec{P}_i^2 - M_0^2 - Re\Sigma^{ret}_{(i)}}{\Gamma_{(i)}}\vec{\nabla}_{X_i}\Gamma_{(i)}\right],$$

$$\frac{d\epsilon_i}{dt} = \frac{1}{1-C_{(i)}}\frac{1}{2\epsilon_i}\left[\frac{\partial Re\Sigma^{ret}_{(i)}}{\partial t} + \frac{\epsilon_i^2 - \vec{P}_i^2 - M_0^2 - Re\Sigma^{ret}_{(i)}}{\Gamma_{(i)}}\frac{\partial\Gamma_{(i)}}{\partial t}\right],$$

with $F_{(i)} \equiv F(t, \vec{X}_i(t), \vec{P}_i(t), \epsilon_i(t))$

$$C_{(i)} = \frac{1}{2\epsilon_i}\left[\frac{\partial}{\partial\epsilon_i} Re\Sigma^{ret}_{(i)} + \frac{\epsilon_i^2 - \vec{P}_i^2 - M_0^2 - Re\Sigma^{ret}_{(i)}}{\Gamma_{(i)}}\frac{\partial}{\partial\epsilon_i}\Gamma_{(i)}\right]$$

Collision term in off-shell transport models

Collision term for reaction 1+2->3+4:

$$I_{coll}(X,\vec{P},M^2) = Tr_2 Tr_3 Tr_4 A(X,\vec{P},M^2)A(X,\vec{P}_2,M_2^2)A(X,\vec{P}_3,M_3^2)A(X,\vec{P}_4,M_4^2)$$

$$|G((\vec{P},M^2)+(\vec{P}_2,M_2^2)\rightarrow(\vec{P}_3,M_3^2)+(\vec{P}_4,M_4^2))|^2_{\mathcal{A},\mathcal{S}}\ \delta^{(4)}(P+P_2-P_3-P_4)$$

$$[\,N_{X\vec{P}_3M_3^2}\,N_{X\vec{P}_4M_4^2}\,\bar{f}_{X\vec{P}M^2}\,\bar{f}_{X\vec{P}_2M_2^2} \;-\; N_{X\vec{P}M^2}\,N_{X\vec{P}_2M_2^2}\,\bar{f}_{X\vec{P}_3M_3^2}\,\bar{f}_{X\vec{P}_4M_4^2}\,]$$

‚gain' term ‚loss' term

with $\bar{f}_{X\vec{P}M^2} = 1+\eta\, N_{X\vec{P}M^2}$ and $\eta = \pm 1$ for bosons/fermions, respectively.

The trace over particles 2,3,4 reads explicitly

for fermions

$$Tr_2 = \sum_{\sigma_2,\tau_2}\frac{1}{(2\pi)^4}\int d^3P_2 \frac{dM_2^2}{2\sqrt{\vec{P}_2^2+M_2^2}}$$

for bosons

$$Tr_2 = \sum_{\sigma_2,\tau_2}\frac{1}{(2\pi)^4}\int d^3P_2 \frac{dP_{0,2}^2}{2}$$

additional integration

The transport approach and the particle spectral functions are fully determined once the in-medium transition amplitudes G are known in their off-shell dependence!

Parton-Hadron-String-Dynamics (PHSD)

PHSD is a non-equilibrium microscopic transport approach for the description of strongly-interacting hadronic and partonic matter created in heavy-ion collisions

Dynamics: based on the solution of generalized off-shell transport equations derived from Kadanoff-Baym many-body theory

Initial A+A collision

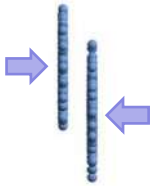

Partonic phase

Hadronization

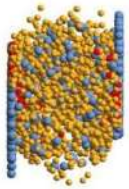

Hadronic phase

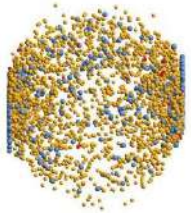

- **Initial A+A collisions :**
  N+N → string formation → decay to pre-hadrons + leading hadrons

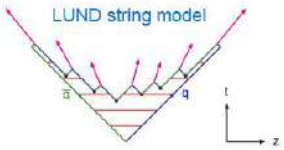

- **Formation of QGP stage if local $\varepsilon > \varepsilon_{critical}$:**
  dissolution of pre-hadrons → partons

- **Partonic phase - QGP:**
  QGP is described by the Dynamical QuasiParticle Model (DQPM) matched to reproduce lattice QCD EoS for finite T and μ_B (crossover)

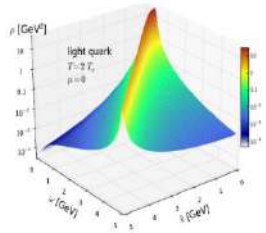

- Degrees-of-freedom: strongly interacting quasiparticles: massive quarks and gluons (g,q,q_{bar}) with sizeable collisional widths in a self-generated mean-field potential

- Interactions: (quasi-)elastic and inelastic collisions of partons

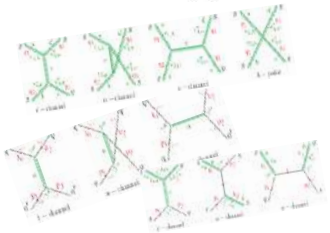

- **Hadronization to colorless off-shell mesons and baryons:**
  Strict 4-momentum and quantum number conservation

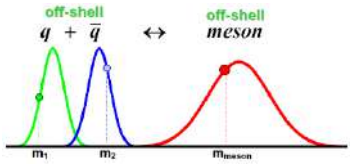

- **Hadronic phase: hadron-hadron interactions – off-shell HSD**

W. Cassing, E. Bratkovskaya, PRC 78 (2008) 034919; NPA831 (2009) 215; W. Cassing, EPJ ST 168 (2009) 3

Traces of the QGP in observables in high energy heavy-ion collisions

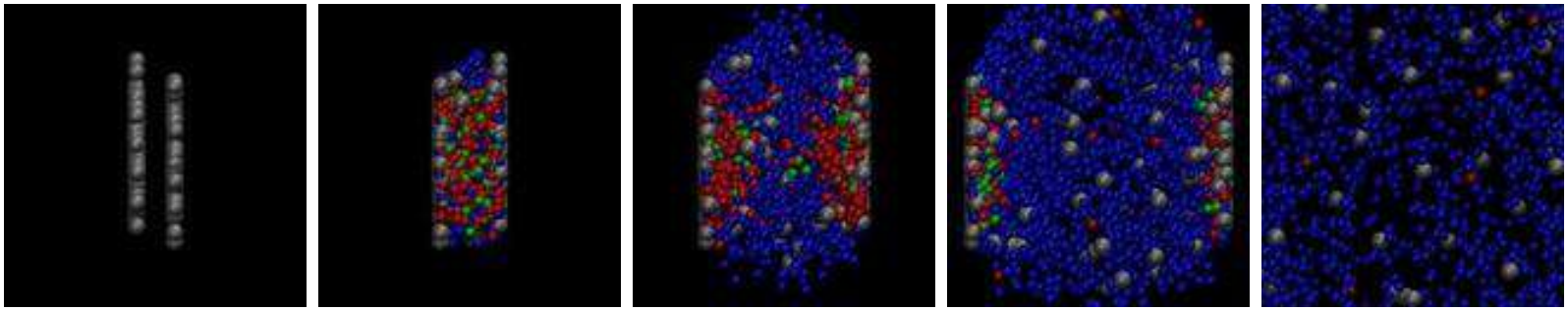

Stages of a collision in PHSD

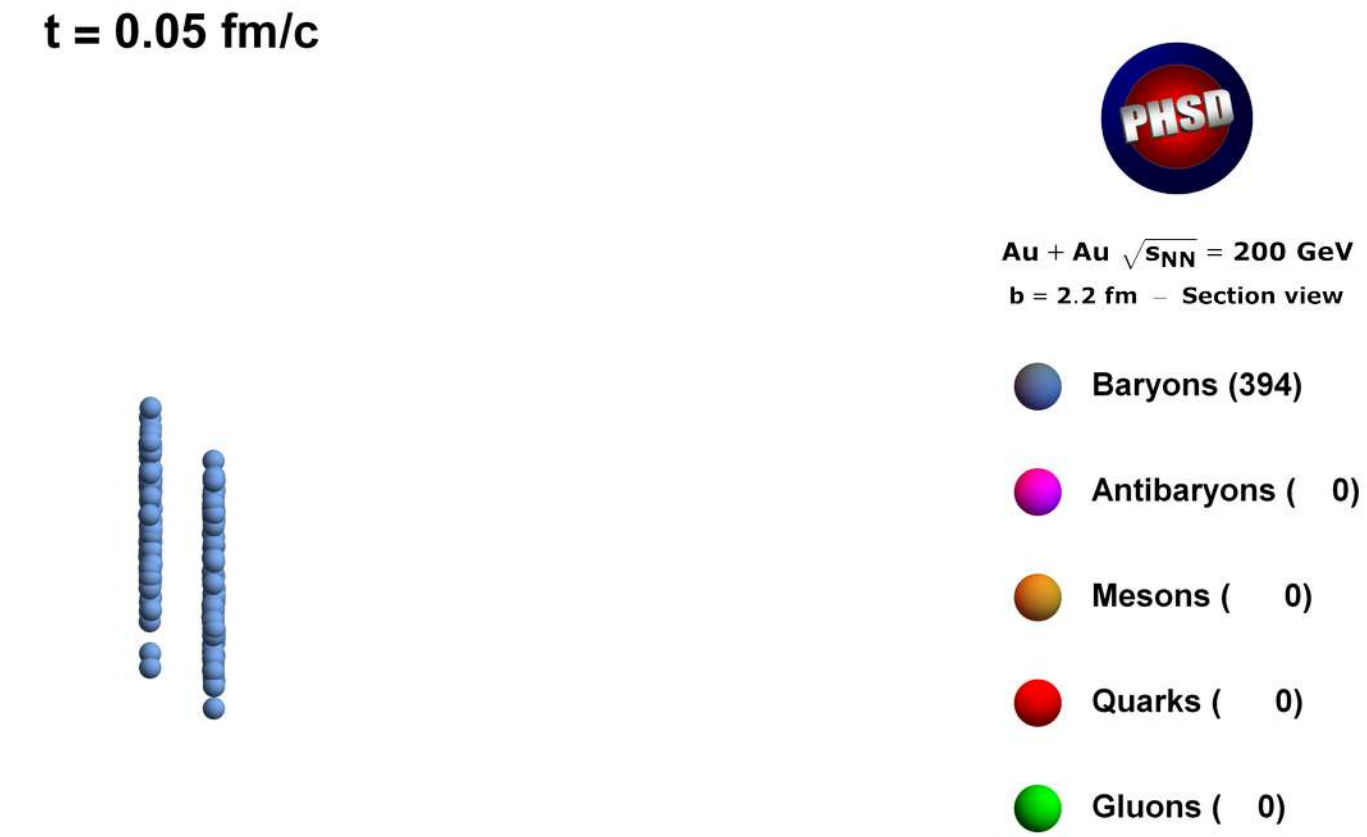

Stages of a collision in PHSD

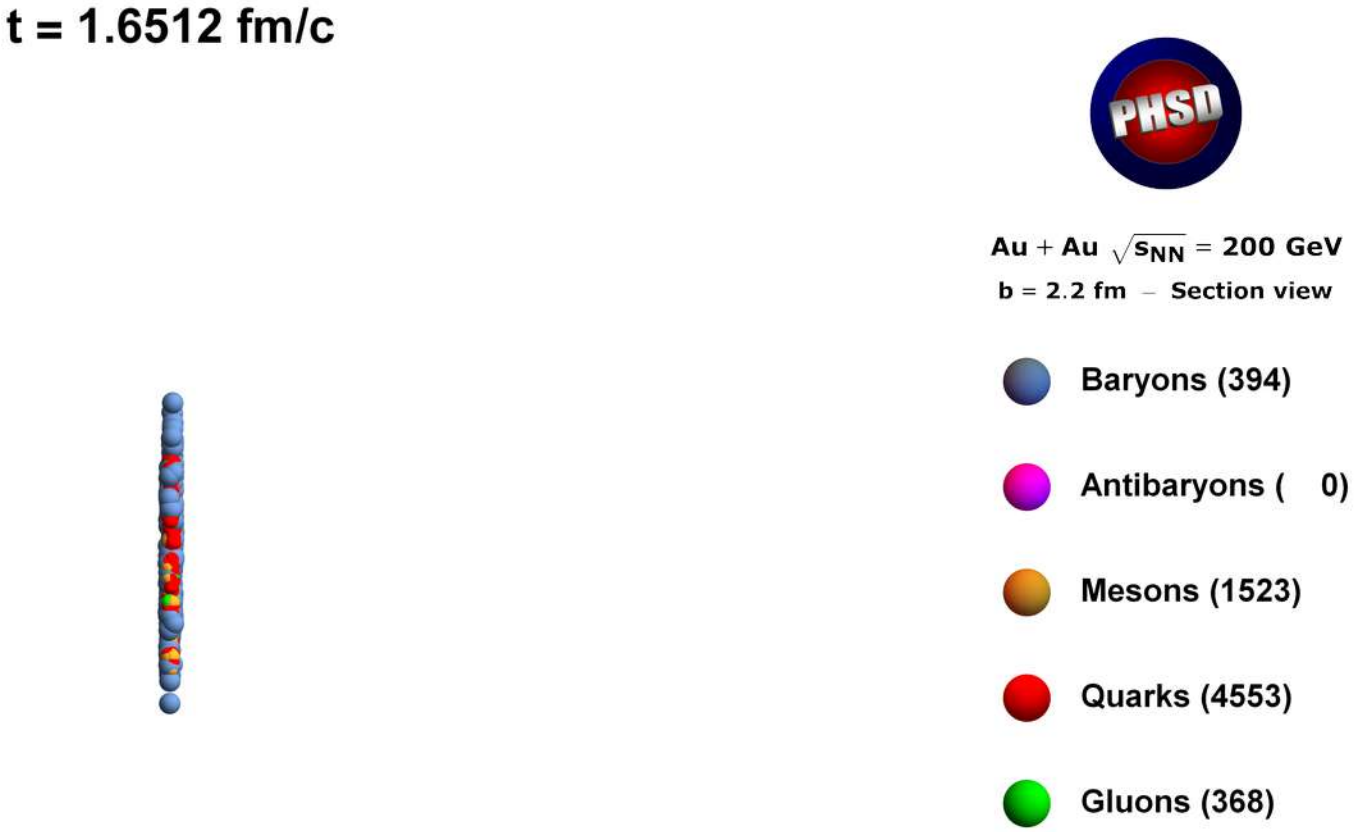

Stages of a collision in PHSD

t = 3.91921 fm/c

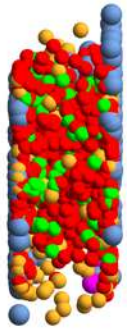

PHSD

Au + Au $\sqrt{s_{NN}}$ = 200 GeV

b = 2.2 fm – Section view

Baryons (426)

Antibaryons (29)

Mesons (1189)

Quarks (4459)

Gluons (783)

Stages of a collision in PHSD

t = 7.31921 fm/c

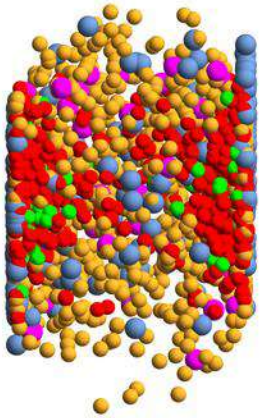

PHSD

Au + Au $\sqrt{s_{NN}}$ = 200 GeV

b = 2.2 fm – Section view

Baryons (540)

Antibaryons (120)

Mesons (2481)

Quarks (2901)

Gluons (492)

Stages of a collision in PHSD

t = 12.0192 fm/c

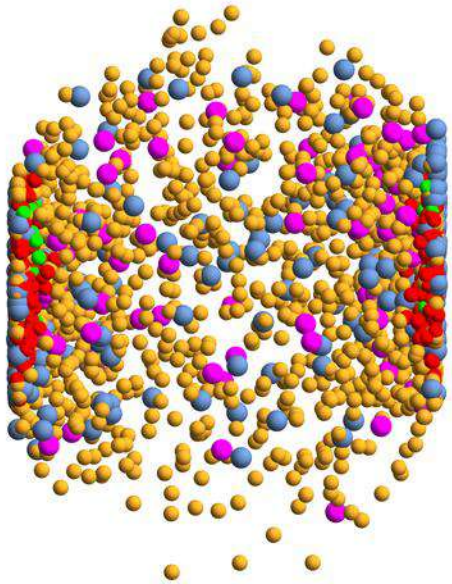

PHSD

Au + Au $\sqrt{s_{NN}}$ = 200 GeV

b = 2.2 fm – Section view

Baryons (626)

Antibaryons (202)

Mesons (3357)

Quarks (1835)

Gluons (269)

Stages of a collision in PHSD

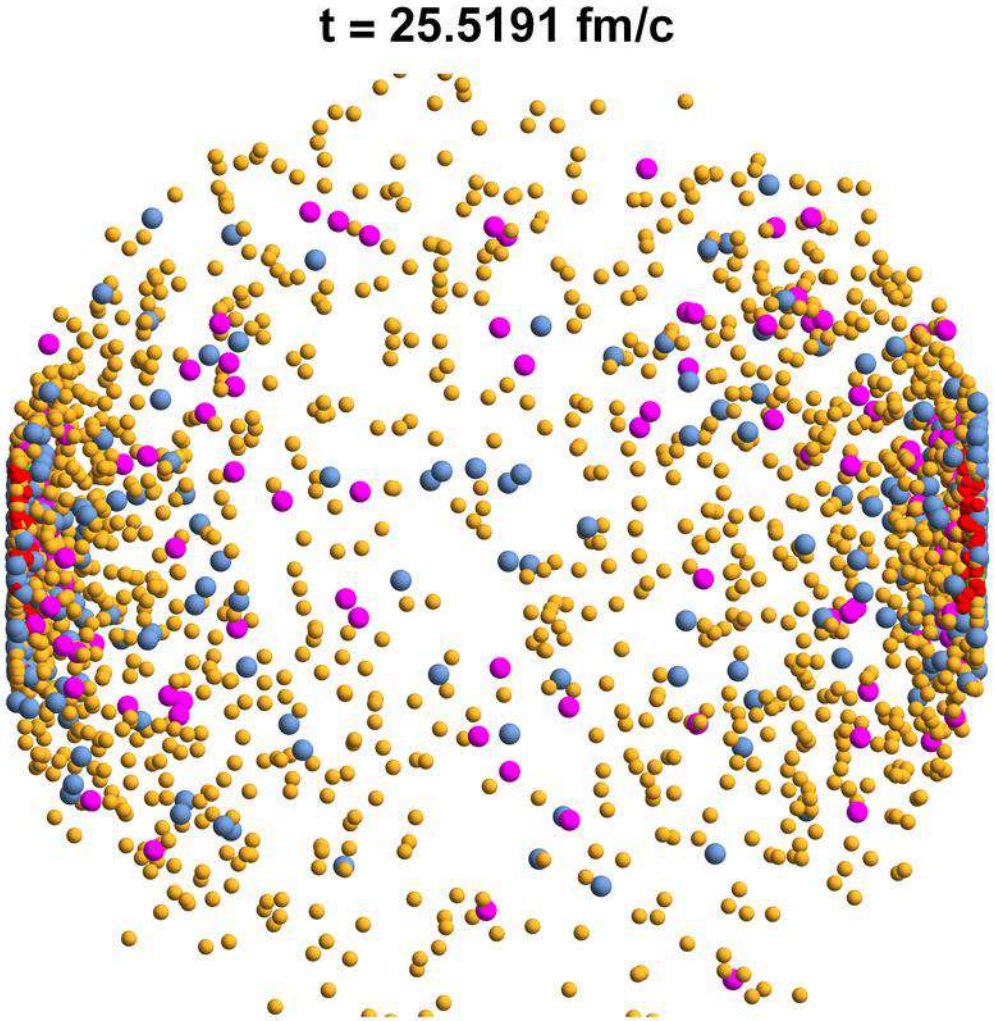

PHSD

Au + Au $\sqrt{s_{NN}}$ = 200 GeV

b = 2.2 fm – Section view

Baryons (710)

Antibaryons (272)

Mesons (4343)

Quarks (899)

Gluons (46)

P.Moreau

Partonic energy fraction in central A+A

Time evolution of the partonic energy fraction vs energy

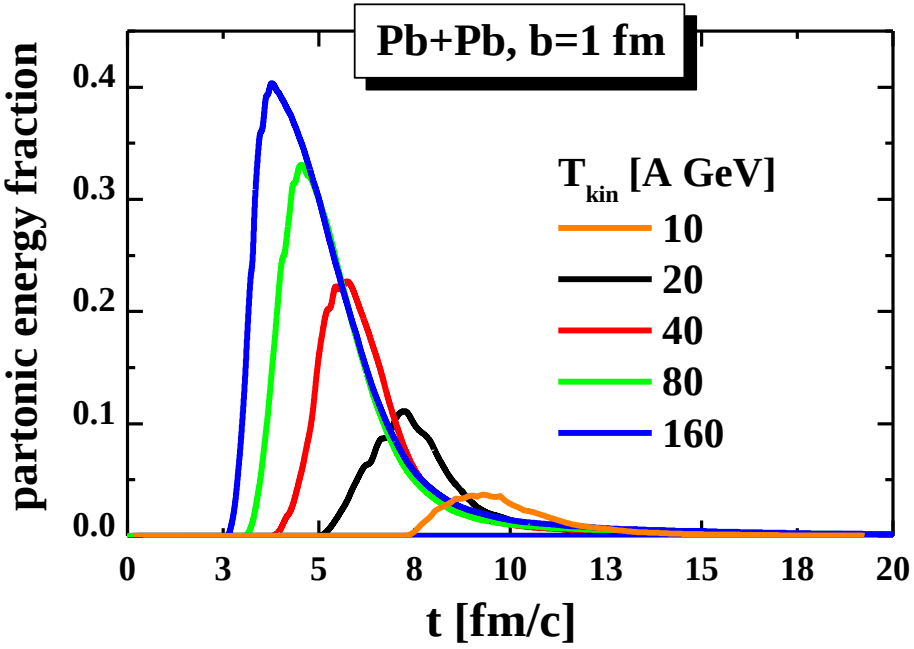

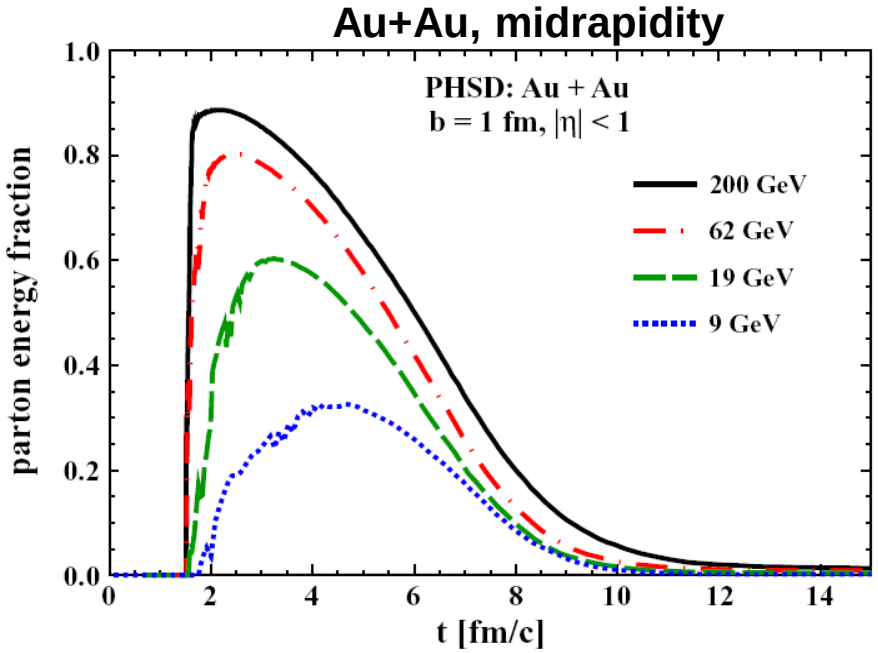

- Strong **increase of partonic phase with energy** from AGS to RHIC

- **SPS:** Pb+Pb, 160 A GeV: only about **40%** of the converted energy goes to partons; the rest is contained in the **large hadronic corona and leading partons**
- **RHIC:** Au+Au, 21.3 A TeV: up to **90%** - **QGP**

W. Cassing & E. Bratkovskaya, NPA 831 (2009) 215
V. Konchakovski et al., Phys. Rev. C 85 (2012) 011902

Time evolution of energy density

PHSD: 1 event Au+Au, 200 GeV, b = 2 fm

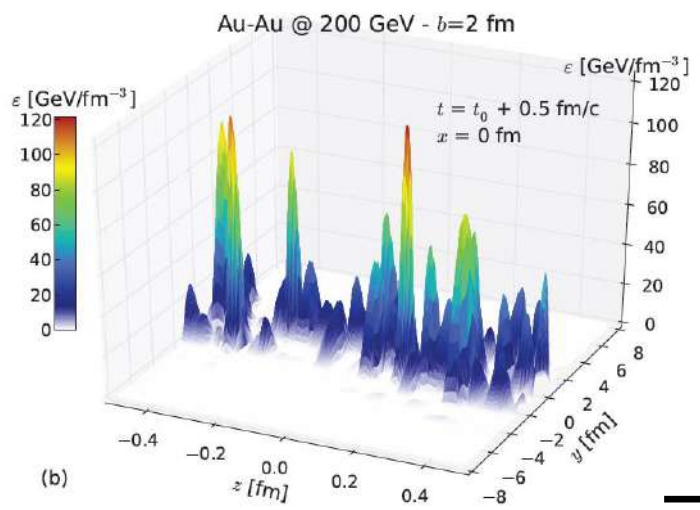

ε(x=0,y,z)

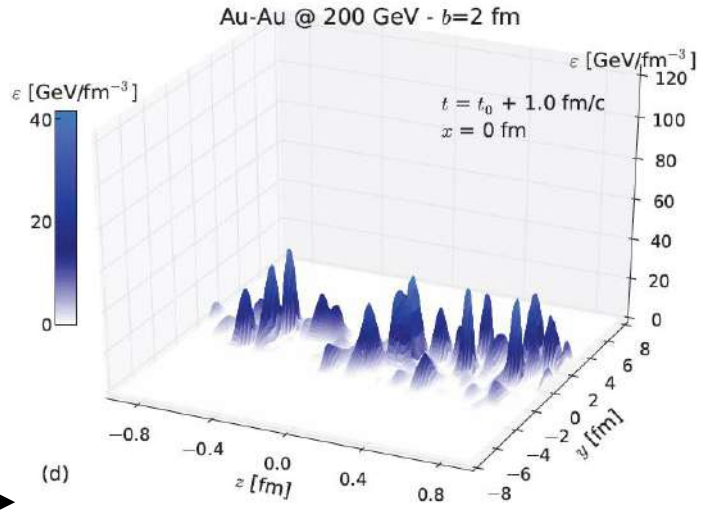

time

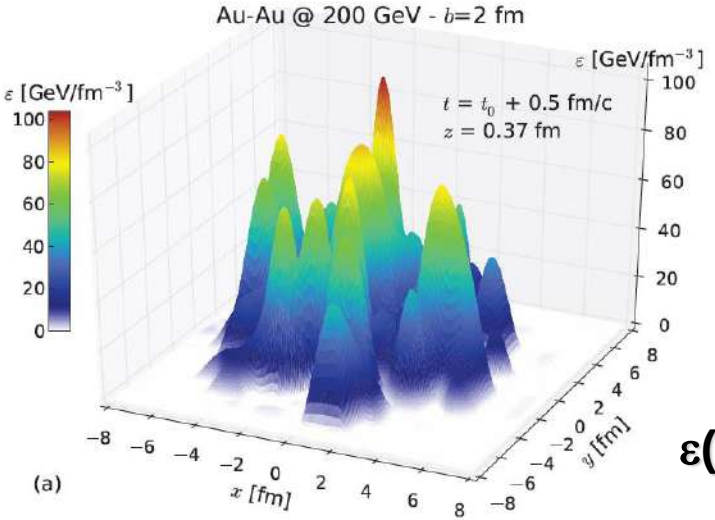

ε(x,y,z=0)

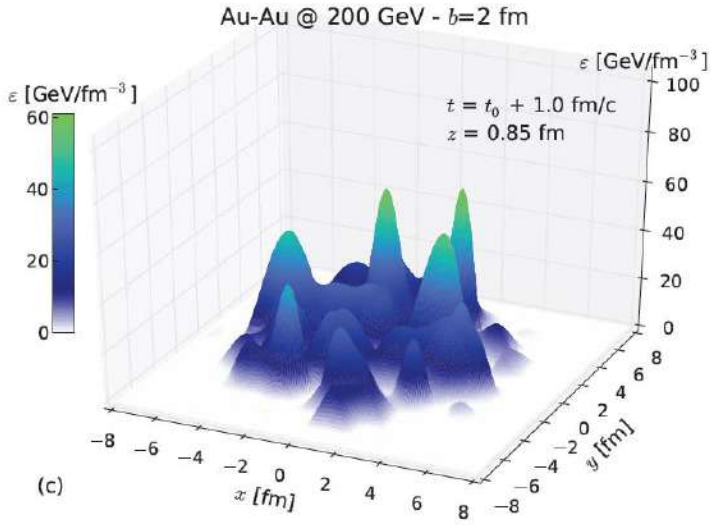

ΔV: Δx=Δy=1fm, Δz=1/γ fm

R. Marty et al., PRC 92 (2015) 015201

Transverse mass spectra from SPS to RHIC

Central Pb + Pb at SPS energies

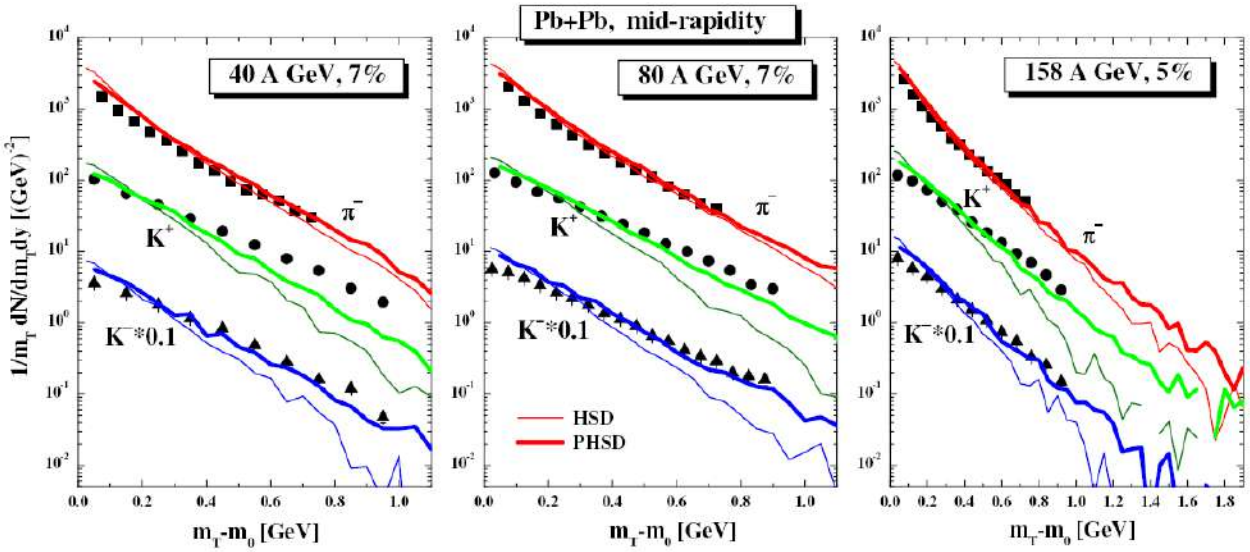

Central Au+Au at RHIC

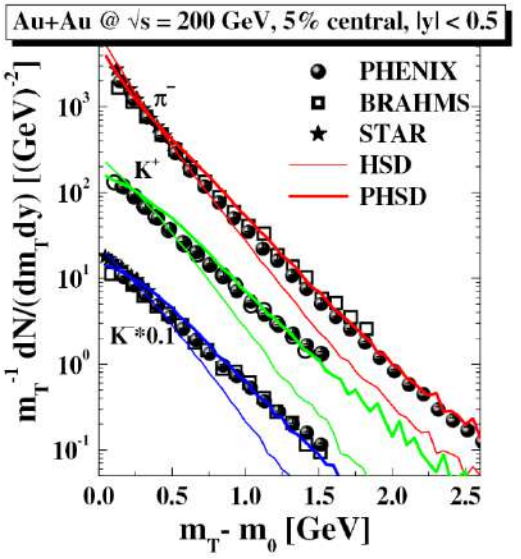

- **PHSD gives harder m_T spectra and works better than HSD (without QGP) at high energies – RHIC, SPS (and top FAIR, NICA)**
- **however, at low SPS (and low FAIR, NICA) energies the effect of the partonic phase decreases due to the decrease of the partonic fraction**

W. Cassing & E. Bratkovskaya, NPA 831 (2009) 215
E. Bratkovskaya, W. Cassing, V. Konchakovski, O. Linnyk, NPA856 (2011) 162

Anisotropy coefficients v_n

Non central Au+Au collisions :

- **interaction between constituents leads to a pressure gradient → spatial asymmetry is converted to an asymmetry in momentum space → collective flow**

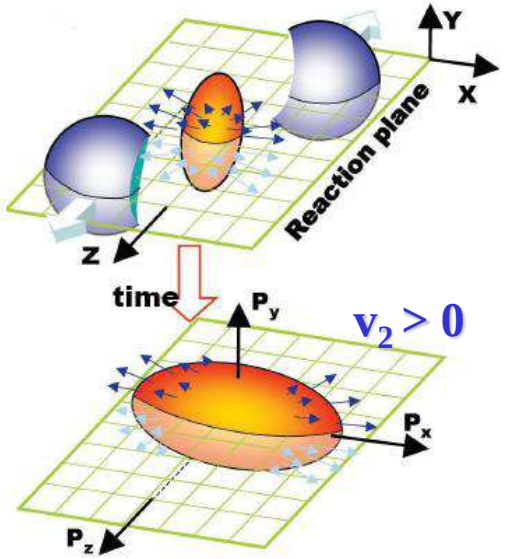

$$\frac{dN}{d\varphi} \propto \left(1 + 2\sum_{n=1}^{+\infty} v_n \cos\left[n(\varphi - \psi_n)\right]\right)$$

$$v_1 = \left\langle \frac{p_x}{p_T} \right\rangle, \quad v_2 = \left\langle \frac{p_x^2 - p_y^2}{p_x^2 + p_y^2} \right\rangle$$

$$v_n = \left\langle \cos n\left(\varphi - \psi_n\right) \right\rangle, \quad n = 1,2,3..,$$

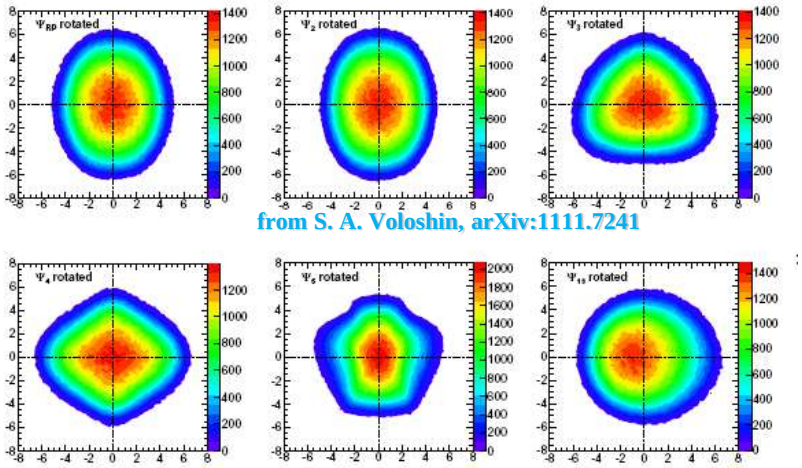

from S. A. Voloshin, arXiv:1111.7241

v_1: directed flow
v_2: elliptic flow
v_3: triangular flow

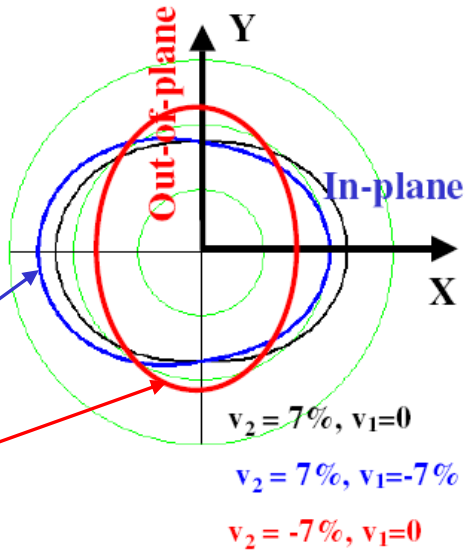

$v_2 > 0$ indicates in-plane emission of particles
$v_2 < 0$ corresponds to a squeeze-out perpendicular to the reaction plane (out-of-plane emission)

Hydrodynamic models: elliptic flow v_2

Comparison between hydro simulations and experimental data for the elliptic flow

Ideal hydrodynamic → **Viscous hydrodynamics**

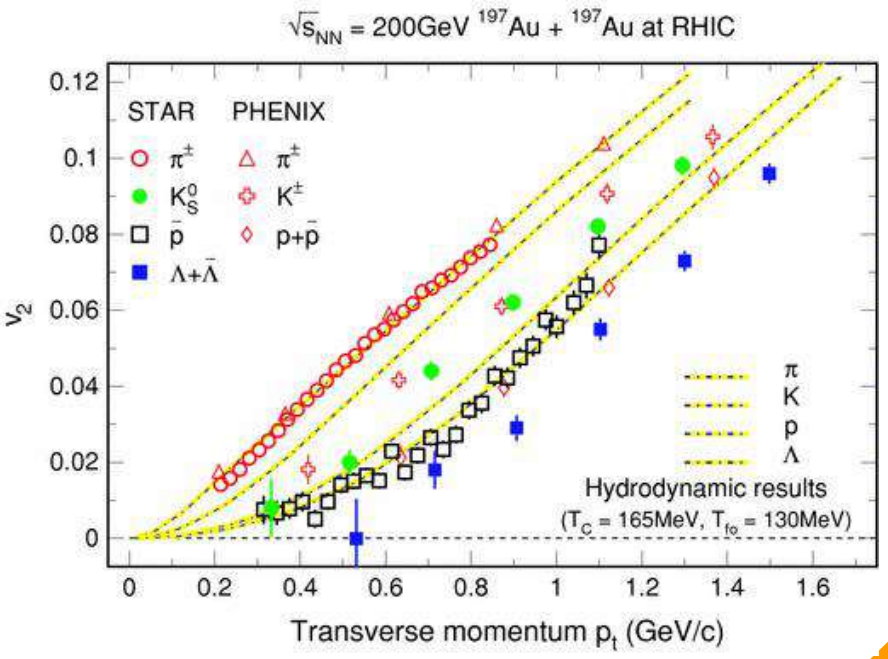

Heinz:2001

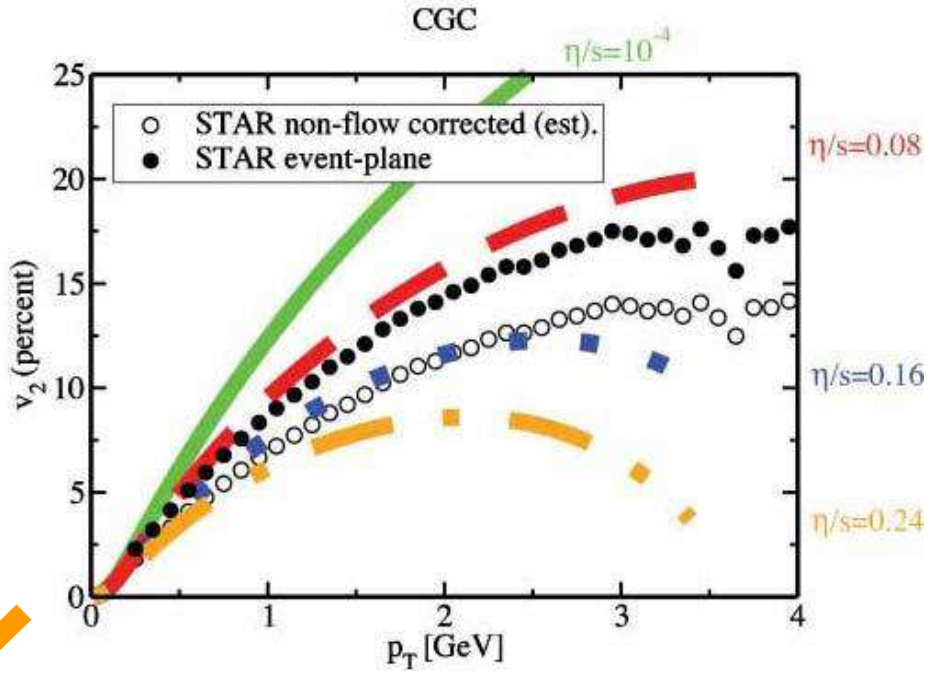

Luzum,Romatschke:2008

Ideal hydro: reproduces exp. data at low p_T, overestimates v_2 at p_T > 1.2 GeV/c

➔ Viscosity of QGP has to be accounted for ➔ viscous hydro

Elliptic flow v_2 is sensitive to η/s

Transport model PHSD: elliptic flow v_2

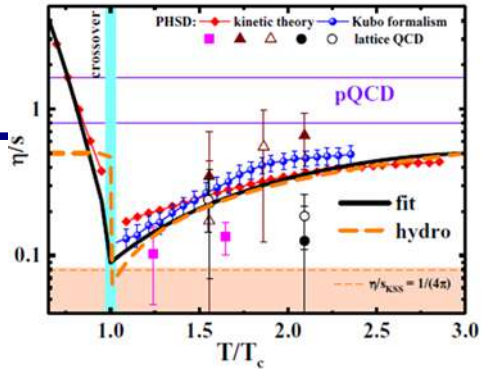

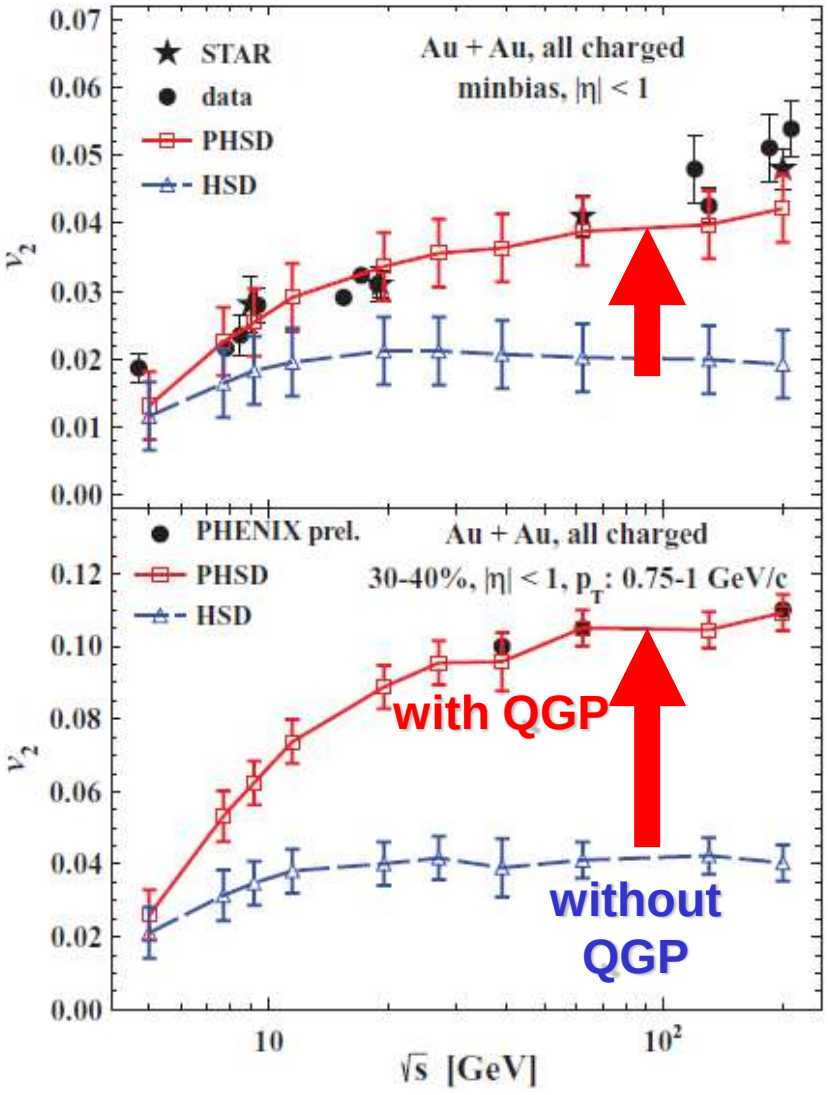

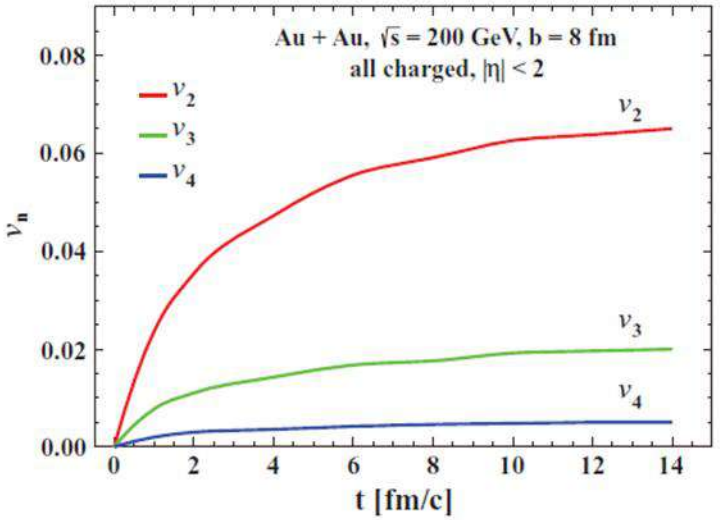

- v_2 in PHSD is larger than in HSD due to the repulsive scalar mean-field potential $U_s(\rho)$ for partons
- v_2 grows with bombarding energy due to the increase of the parton fraction

V. Konchakovski, E. Bratkovskaya, W. Cassing, V. Toneev, V. Voronyuk, Phys. Rev. C 85 (2012) 011902

V_n (n=2,3,4,5) of charged particles from PHSD at LHC

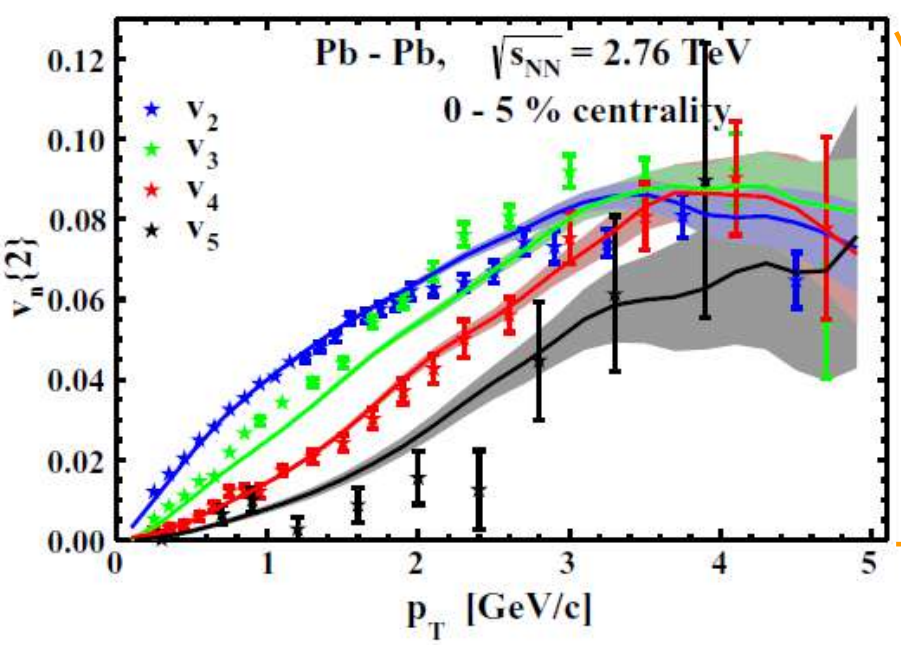

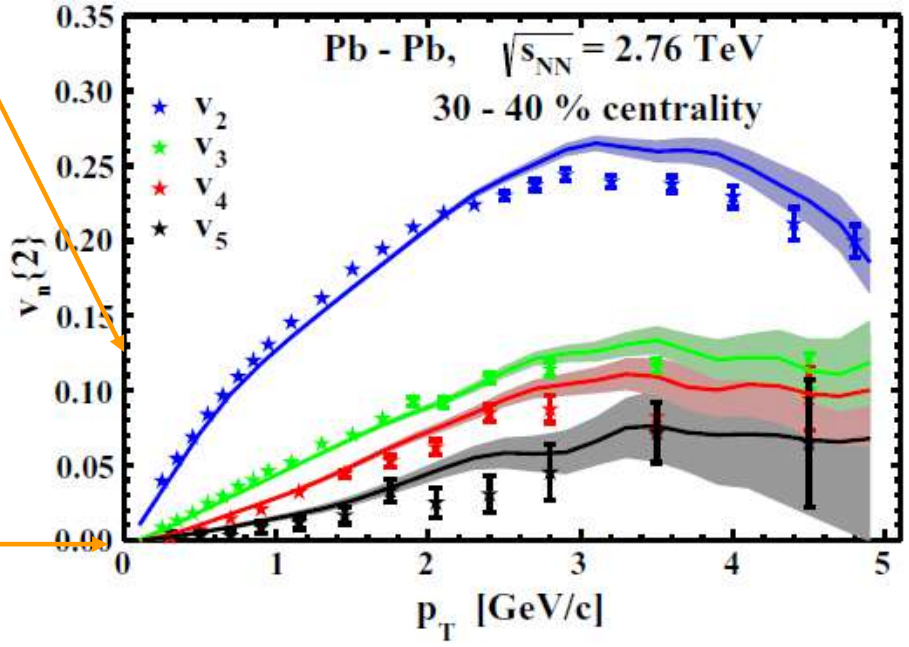

- **PHSD: increase of v_n (n=2,3,4,5) with p_T**
- **v_2 increases with decreasing centrality**
- **v_n (n=3,4,5) show weak centrality dependence**

symbols – ALICE

PRL 107 (2011) 032301

lines – PHSD (e-by-e)

v_n (n=3,4,5) develops by interactions in the QGP and in the final hadronic phase

V. Konchakovski, W. Cassing, V. Toneev, J. Phys. G: Nucl. Part. Phys 42 (2015) 055106

Traces of the QGP at finite μ_q in observables in high energy heavy-ion collisions

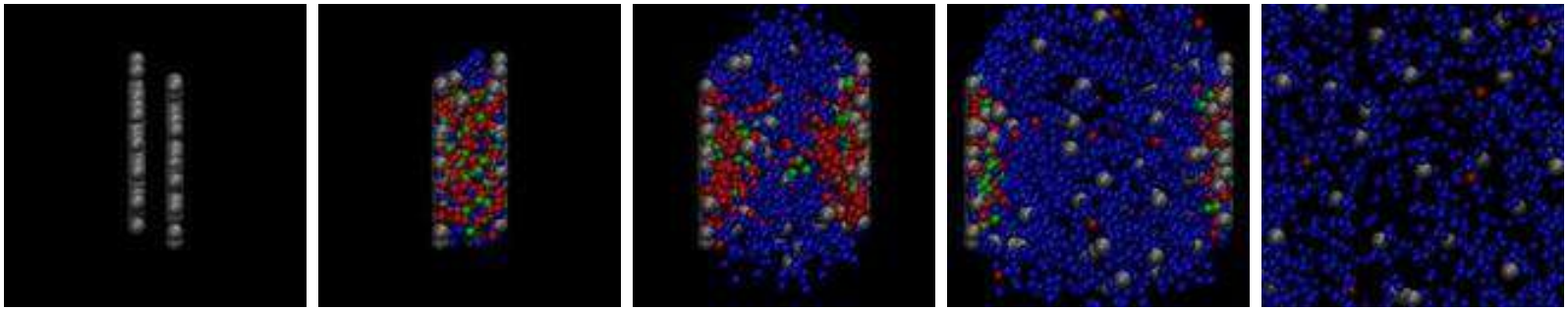

Extraction of (T, μ_B) in PHSD

- **For each cell in PHSD :**
  In order to extract (T, μ_B) use lQCD relations (up to 4th order) - Taylor series :

(1) lQCD

$$\frac{n_B}{T^3} \approx \chi_2^B(T)\left(\frac{\mu_B}{T}\right) + \dots$$

$$\Delta\epsilon/T^4 \approx \frac{1}{2}\left(T\frac{\partial\chi_2^B(T)}{\partial T} + 3\chi_2^B(T)\right)\left(\frac{\mu_B}{T}\right)^2 + \dots$$

*** Use baryon number susceptibilities χ_n from lQCD**

➔ **obtain (T, μ_B) by solving the system of coupled equations using ε^{PHSD} and n_B^{PHSD}**

*** Done by the Newton-Raphson method**

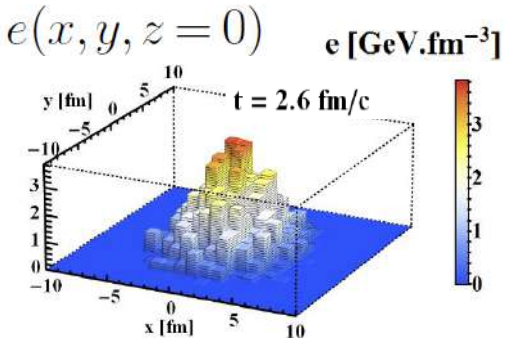

Au+Au, 200 GeV, b=6 fm

Input:

ε^{PHSD} **and** n_B^{PHSD}

(1)

lQCD

Output:

T, μ_B

P. Moreau et al., PRC100 (2019) 014911

Illustration for a HIC ($\sqrt{s_{NN}} = 19.6$ GeV)

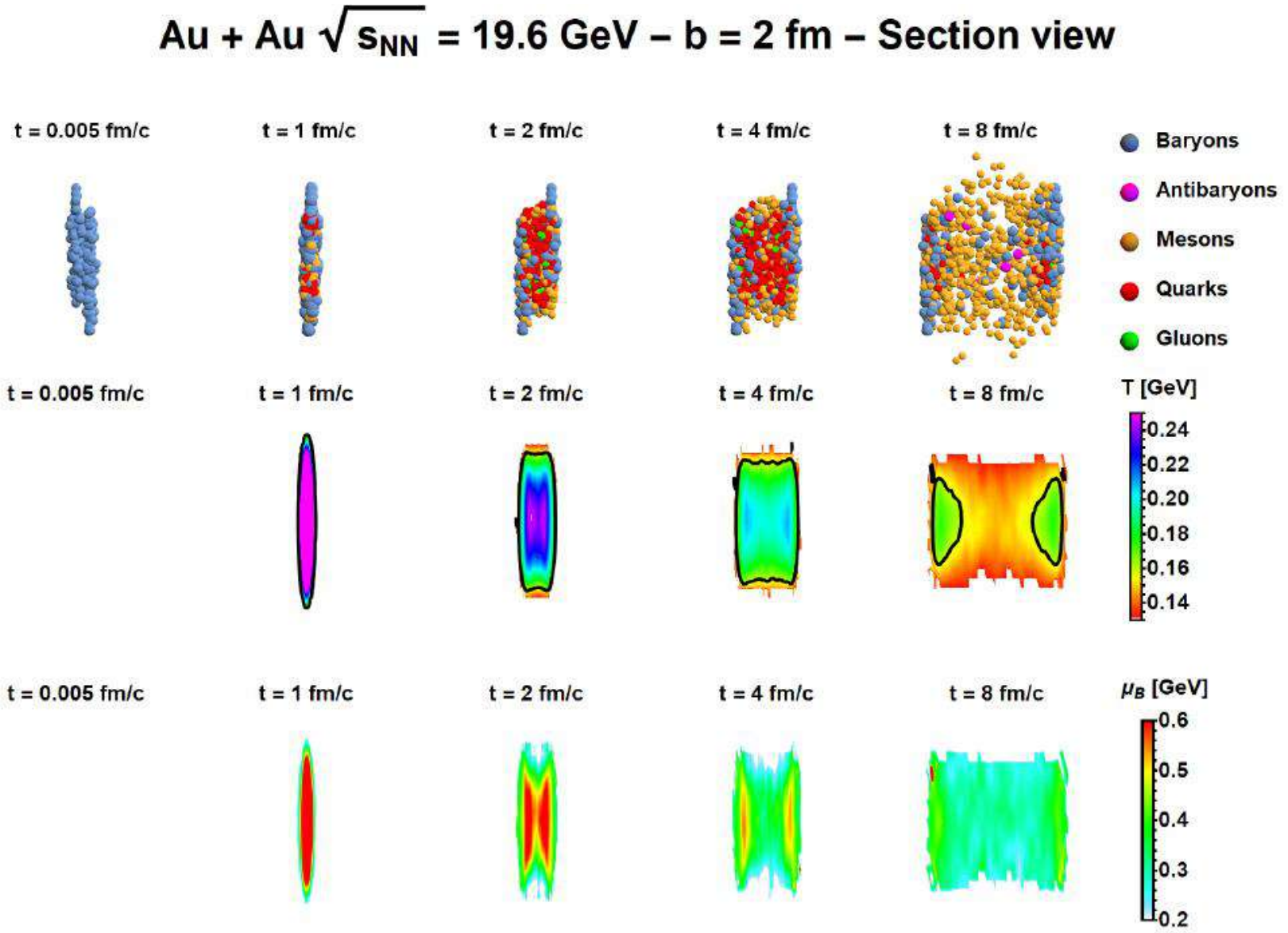

Illustration for a HIC ($\sqrt{s_{NN}} = 17$ GeV)

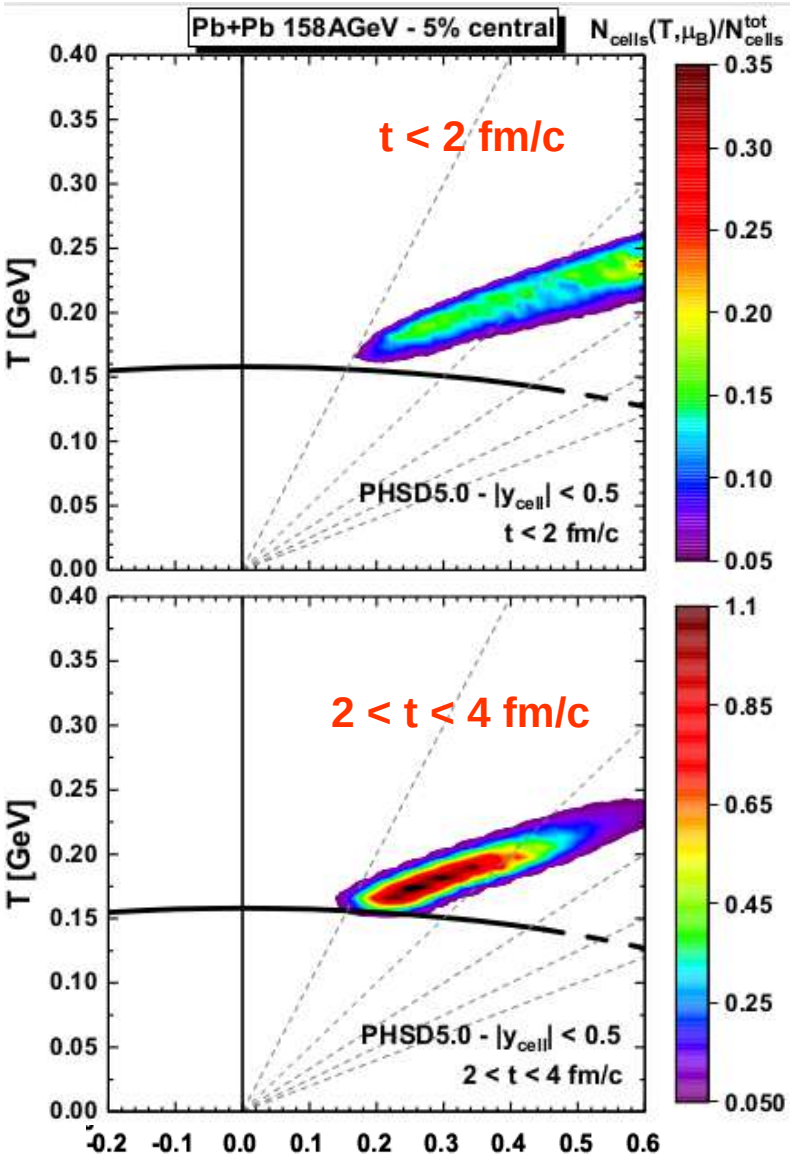

Distribution of cells ($|y_{cell}|$<0.5) with $T>T_C$

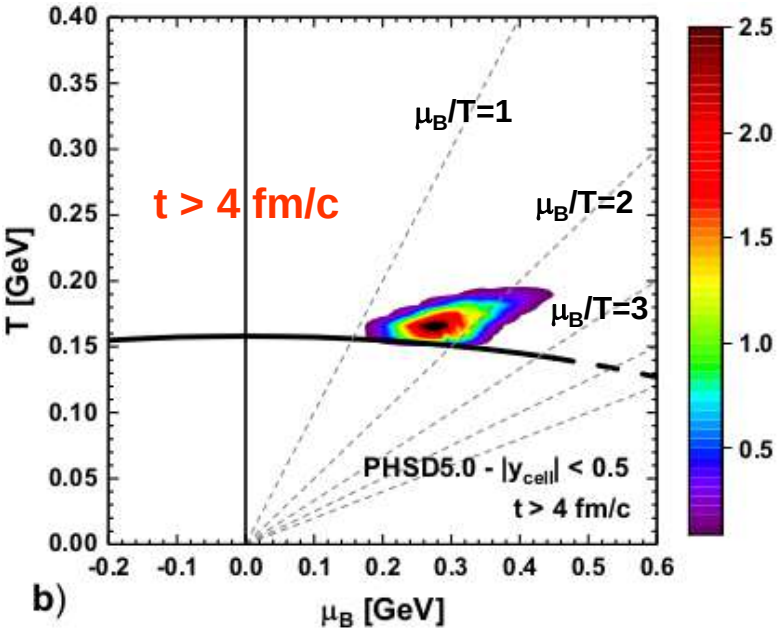

P. Moreau et al., PRC100 (2019) 014911

Results for HICs from PHSD 4.0 and 5.0

➢ **Comparison between three different results:**

1) PHSD 4.0 : only $\sigma(T)$ and $\rho(T)$

$\sigma(T)$ – parton interaction cross sections
$\rho(T)$ – spectral function of partons
➔ (masses and widths)

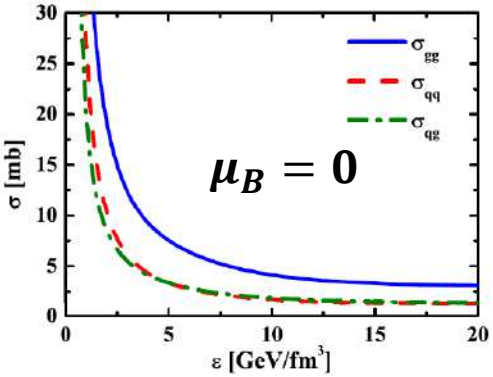

2) PHSD 5.0 : with $\sigma(\sqrt{s}, m_1, m_2, T, \mu_B = 0)$ and $\rho(T, \mu_B = 0)$

In v.5.0: + angular dependence of diff. partonic cross sections

3) PHSD 5.0 : with $\sigma(\sqrt{s}, m_1, m_2, T, \mu_B)$ and $\rho\ (T, \mu_B)$

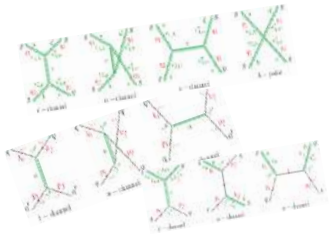

P. Moreau et al., PRC100 (2019) 014911

Results for HICs ($\sqrt{s_{NN}} = 200$ GeV)

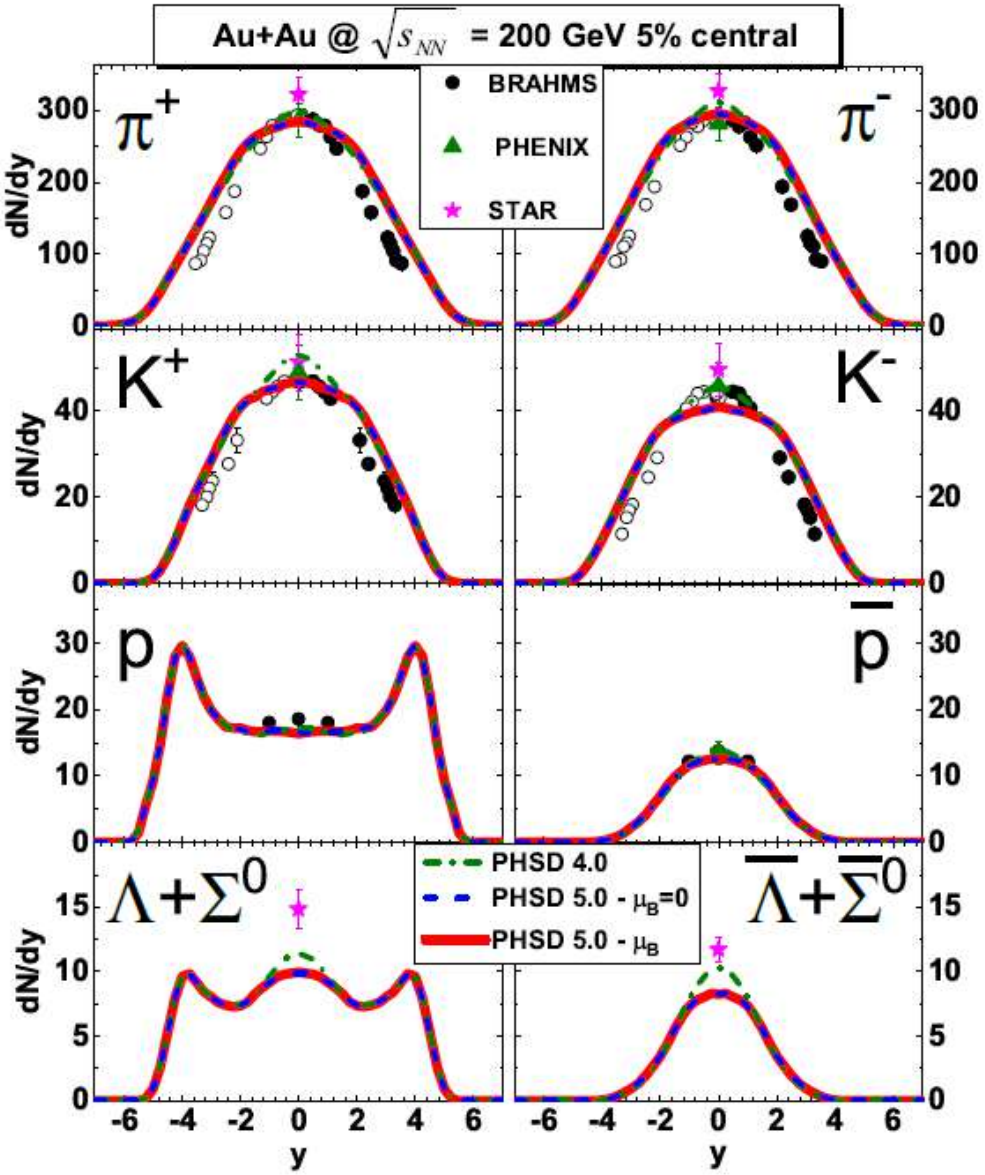

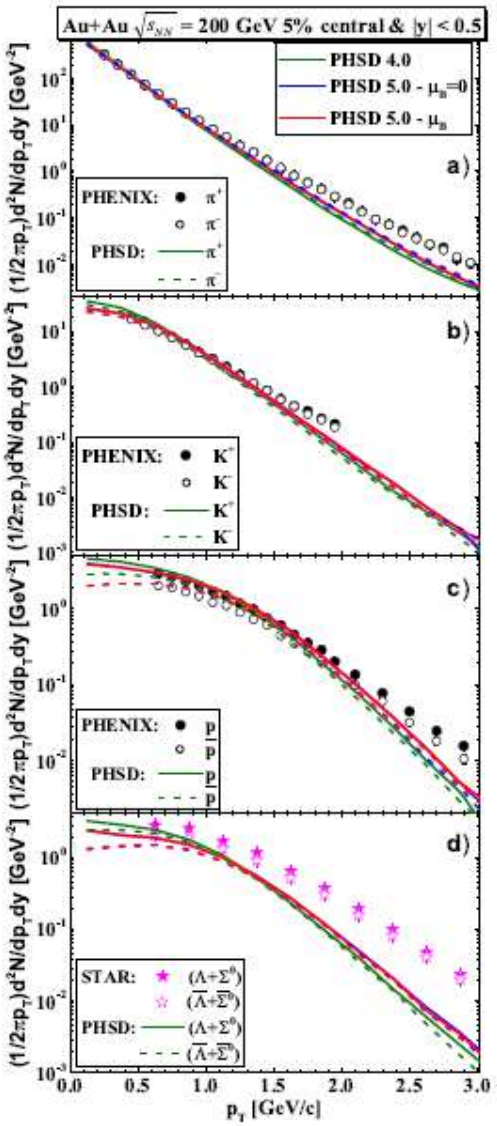

P. Moreau et al., PRC100 (2019) 014911

Results for HICs ($\sqrt{s_{NN}} = 17$ GeV)

High-μ_B regions are probed at low $\sqrt{s_{NN}}$ or high rapidity regions
But, QGP fraction is small at low $\sqrt{s_{NN}}$

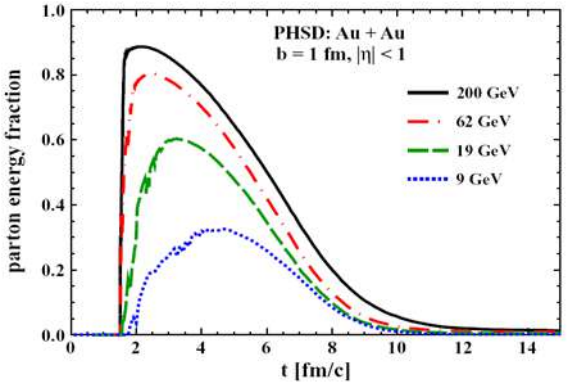

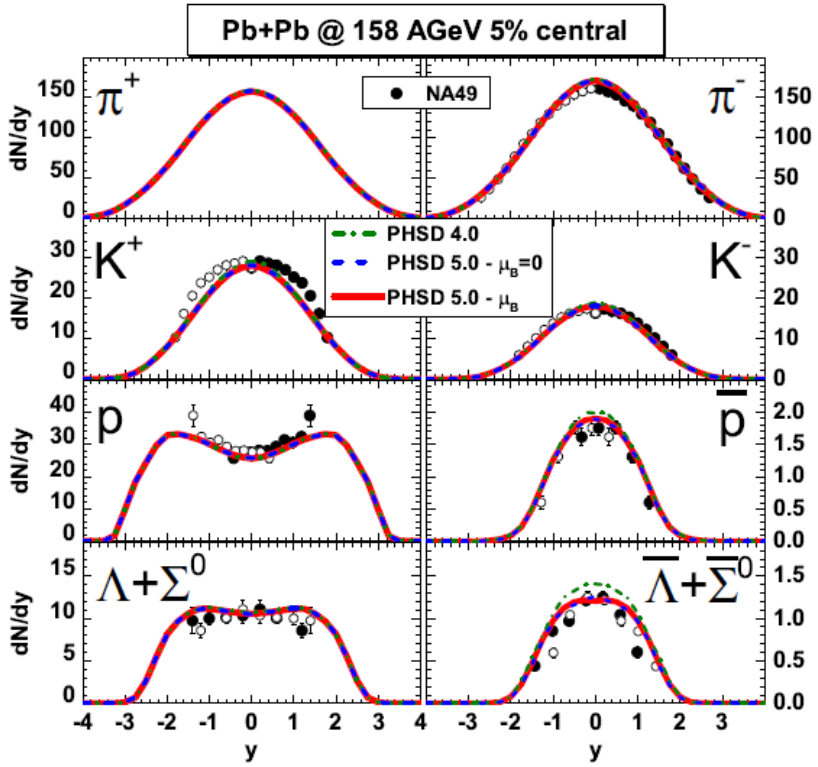

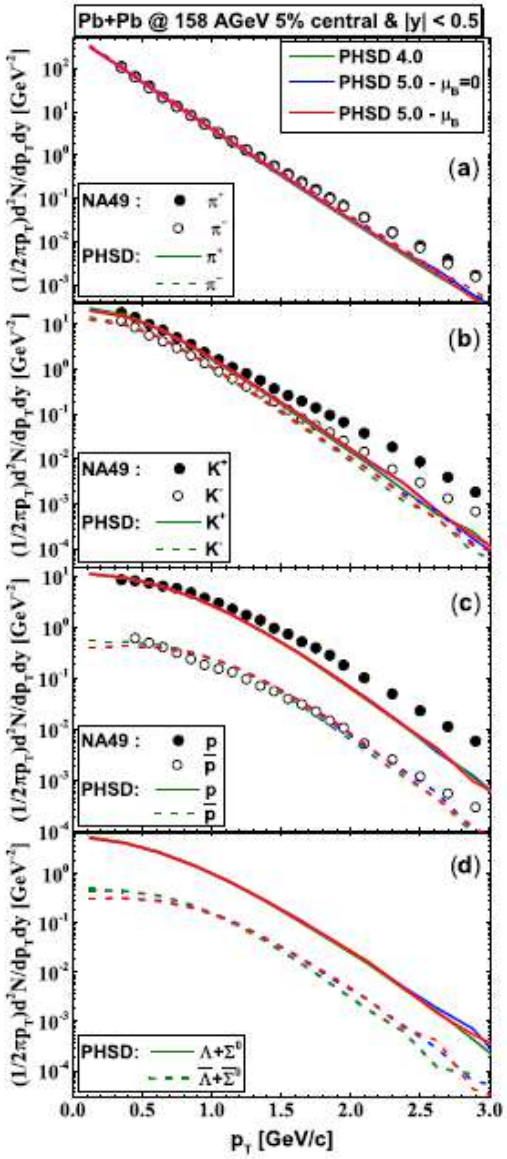

P. Moreau et al., PRC100 (2019) 014911

Results for HICs ($\sqrt{s_{NN}} = 7.6$ GeV)

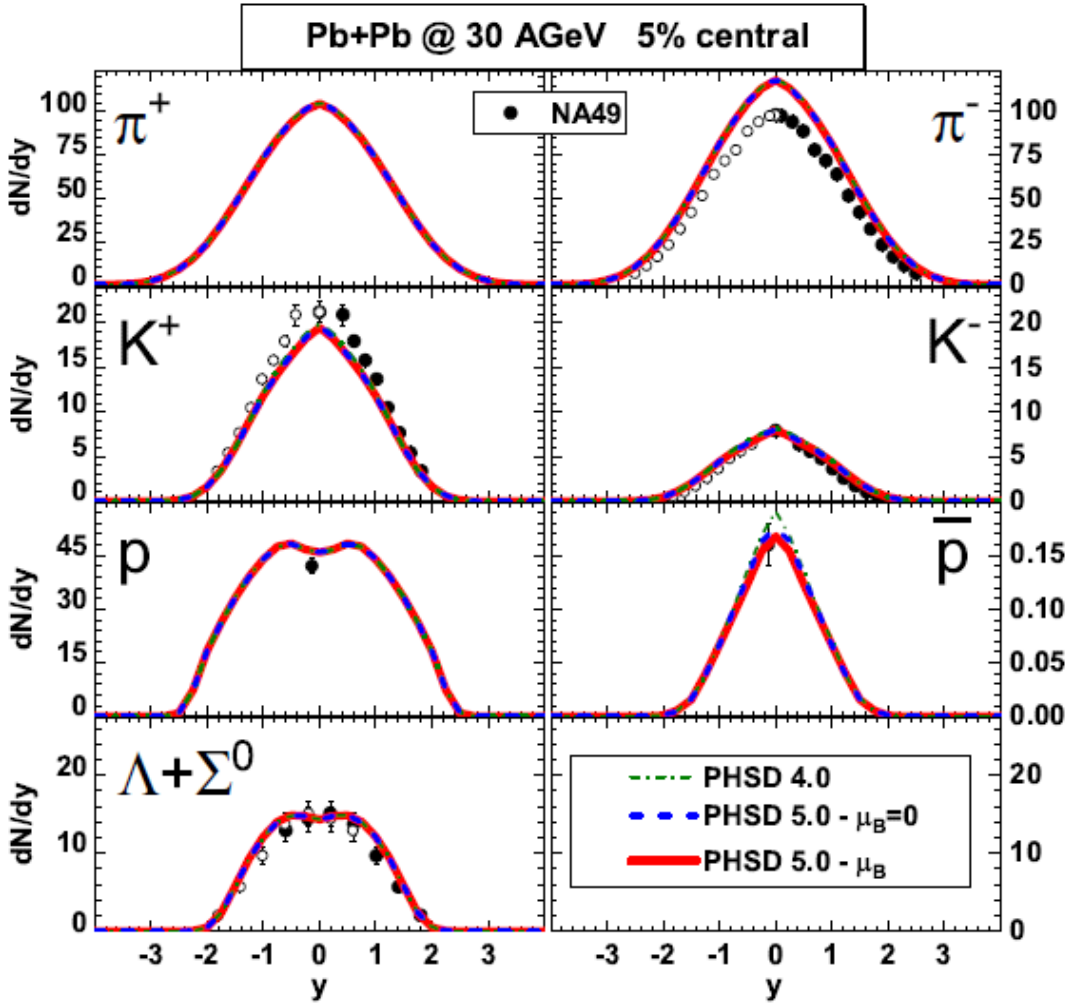

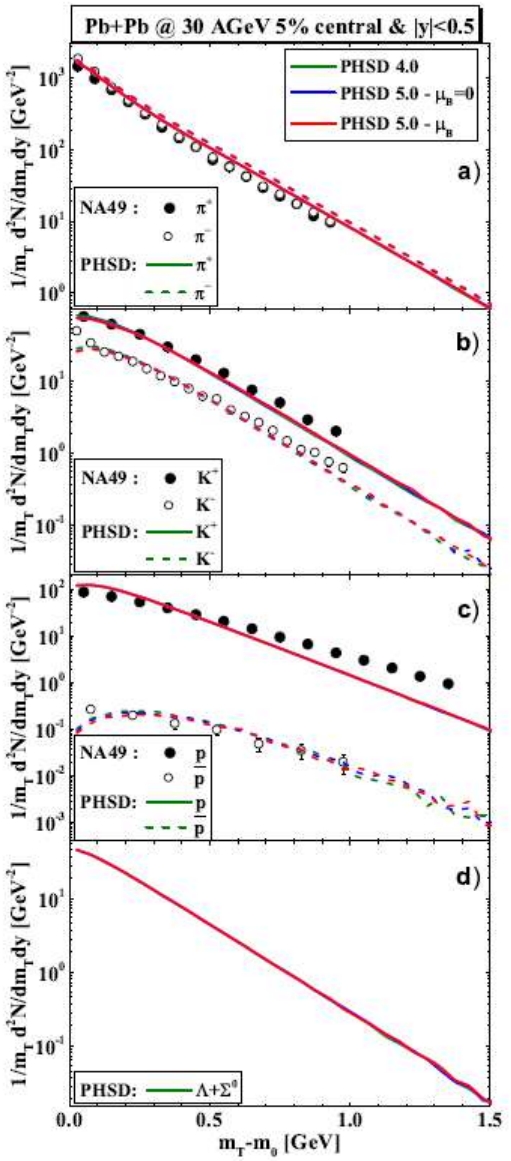

- very **weak dependence** of 'bulk' observables on μ_B

P. Moreau et al., PRC100 (2019) 014911

Results for HICs ($\sqrt{s_{NN}} = 4.86$ GeV)

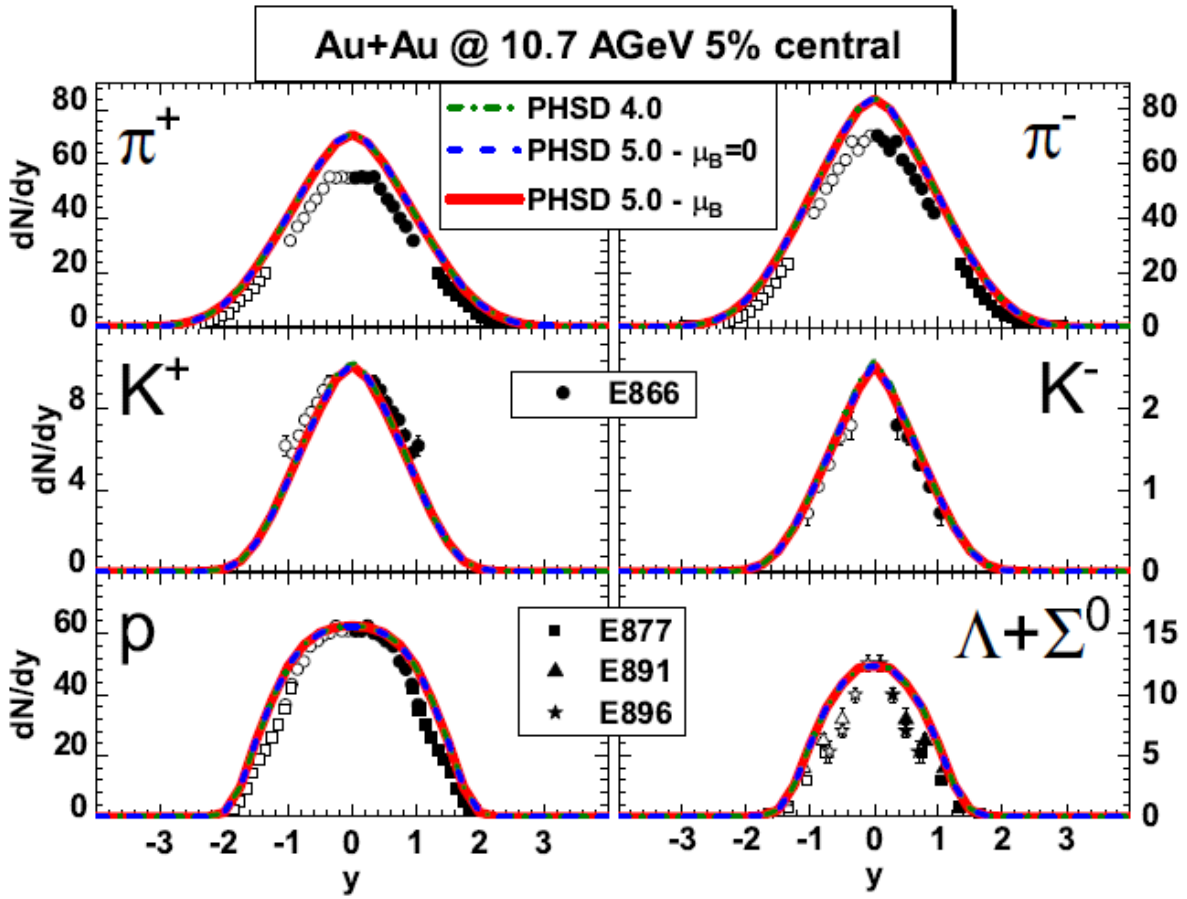

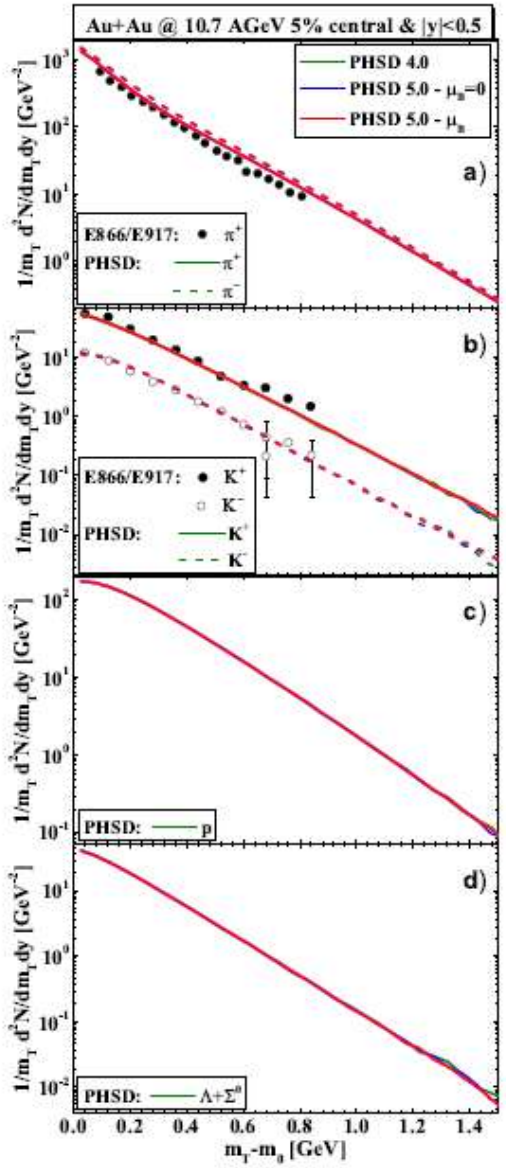

- very weak dependence of 'bulk' observables on μ_B

P. Moreau et al., PRC100 (2019) 014911

Elliptic flow v_2 ($\sqrt{s_{NN}} = 200\ GeV\ vs\ 27 GeV$)

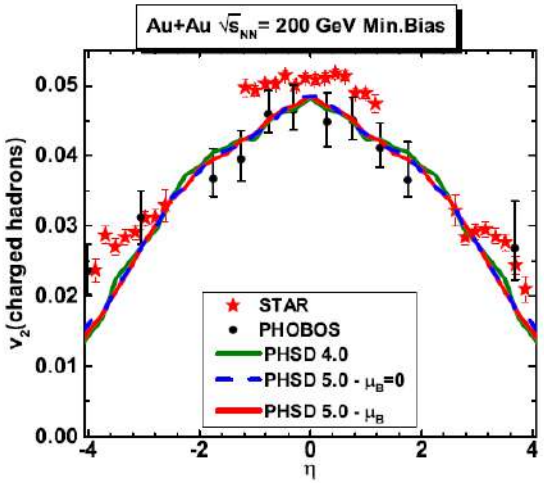

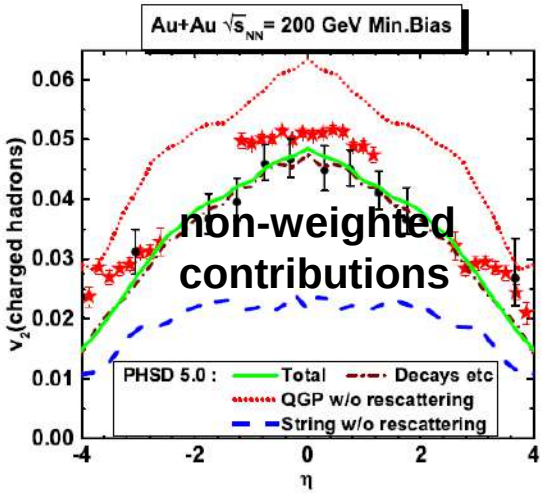

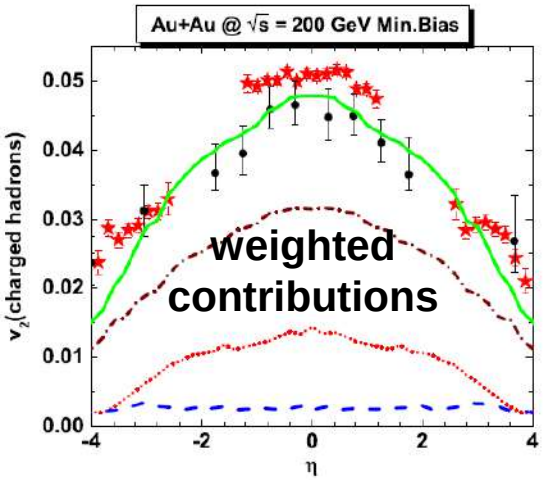

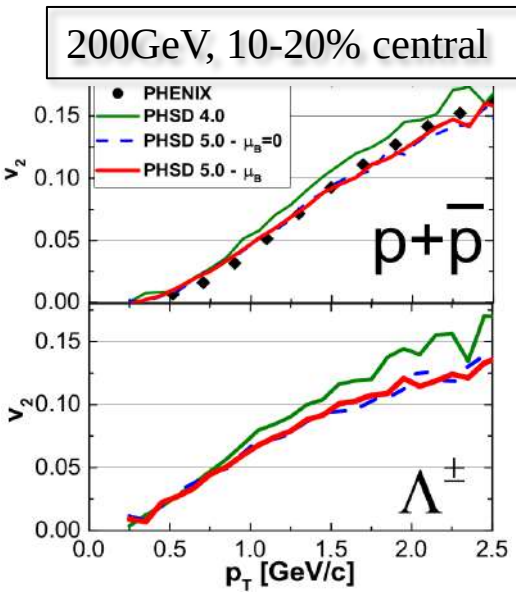

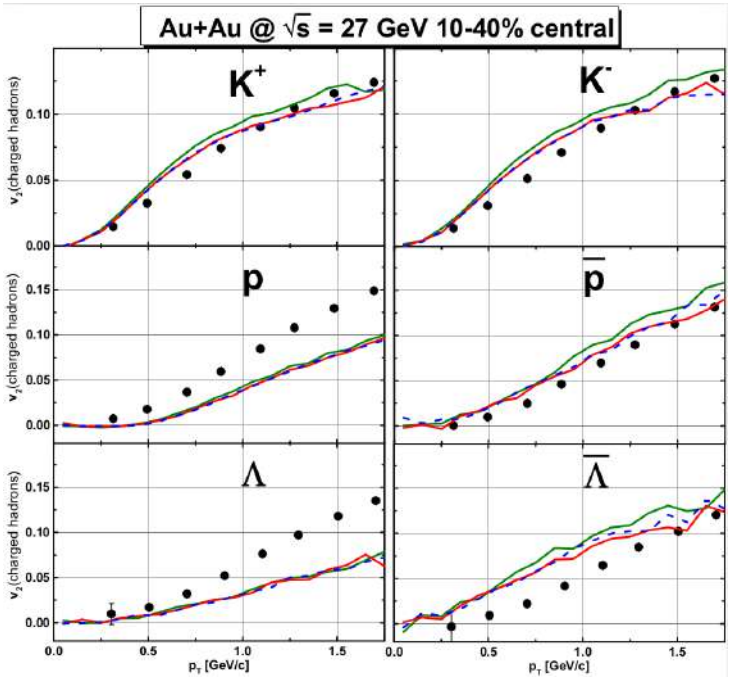

➔ **Small effect of μ_B dependence on v_2**

O. Soloveva et al., arXiv:2001.07951, MDPI Particles 2020, 3, 178

Results for v_1 for HICs ($\sqrt{s_{NN}} = 27$ GeV)

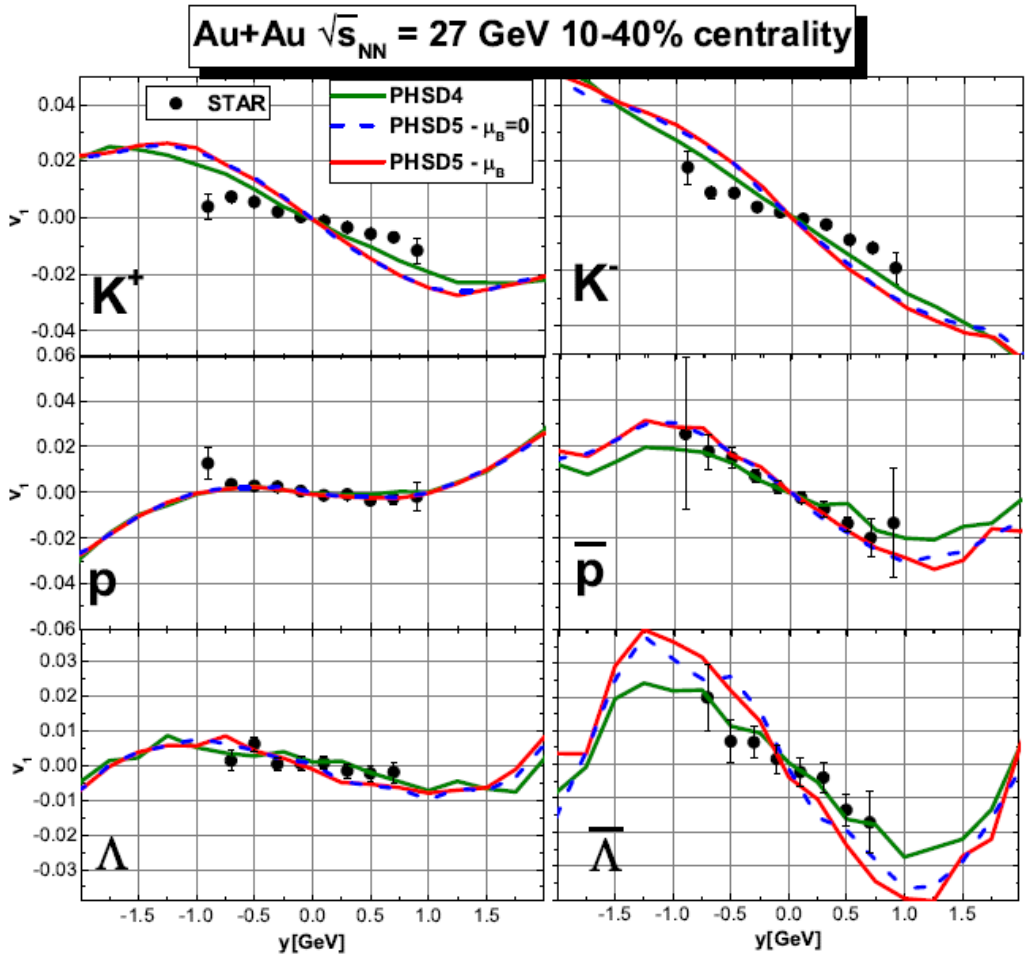

Messages from v_1, v_2 analysis:

- **weak dependence** of v_1, v_2 on μ_B
- **small influence** on v_1, v_2 of explicit $\sqrt{s}$ **-dependence** of total partonic cross sections σ + **angular dependence** of $d\sigma/d\cos\theta$ due to the relatively **small QGP volume**
- strong **flavor dependence** of v_1, v_2

O. Soloveva et al., arXiv:2001.07951, MDPI Particles 2020, 3, 178

Messages from studies of QGP at T,μ_B

- (T, μ_B)-dependent partonic cross sections and masses/widths of quarks and gluons have been implemented in PHSD
- High-μ_B region is probed at low bombarding energies or high rapidity regions
- But, QGP fraction is small at low bombarding energies:
  ➔ no effects of (T, μ_B)-dependent partonic cross sections and masses/widths seen in 'bulk' observables – dN/dy, p_T-spectra
- Flow harmonics v_1, v_2 show :
  visible sensitivity to the explicit $\sqrt{s}$ -dependence of total partonic cross sections σ + angular dependence of $d\sigma/d\cos\theta$, however, weak dependence on μ_B

- **Outlook:**
  - More precise EoS at large μ_B
  - Possible 1st order phase transition at even larger μ_B?!

High-μ_B region of QCD phase diagram ➔ challenge for FAIR, NICA, BES RHIC

Thanks to:

PHSD group - 2021

GSI & Frankfurt University
Olga Soloveva, Taesoo Song, Lucia Oliva,
Gabriele Coci, Ilia Grishmanovskii, Elena Bratkovskaya

Giessen University: Wolfgang Cassing

Former group members:

Olena Linnyk
Vitalii Ozvenchuk
Volodya Konchakovski
Hamza Berrehrah
Rudy Marty
Pierre Moreau
Thorsten Steinert
Alessia Palmese
Eduard Seifert
Andrej Ilner
Daniel Cabrera

Collaborations:

Frankfurt University:
Carsten Greiner, Juan Torres-Rincon

SUBATECH, Nantes University:
Jörg Aichelin, Pol-Bernard Gossiaux,
Marlene Nahrgang, Klaus Werner

JINR, Dubna:
Vadim Voronyuk, Viktor Kireev

Barcelona University:
Laura Tolos

Duke University:
Steffen Bass, Pierre Moreau

Catania University:
Vincenzo Greco

PHSD home page:
http://theory.gsi.de/~ebratkov/phsd-project/PHSD/index1.html